

Generalized Weyl solutions in $d = 5$ Einstein-Gauss-Bonnet theory: the static black ring

Burkhard Kleihaus, Jutta Kunz and Eugen Radu

Institut für Physik, Universität Oldenburg, Postfach 2503 D-26111 Oldenburg, Germany

ABSTRACT: We argue that the Weyl coordinates and the rod-structure employed to construct static axisymmetric solutions in higher dimensional Einstein gravity can be generalized to the Einstein-Gauss-Bonnet theory. As a concrete application of the general formalism, we present numerical evidence for the existence of static black ring solutions in Einstein-Gauss-Bonnet theory in five spacetime dimensions. They approach asymptotically the Minkowski background and are supported against collapse by a conical singularity in the form of a disk. An interesting feature of these solutions is that the Gauss-Bonnet term reduces the conical excess of the static black rings. Analogous to the Einstein-Gauss-Bonnet black strings, for a given mass the static black rings exist up to a maximal value of the Gauss-Bonnet coupling constant α' . Moreover, in the limit of large ring radius, the suitably rescaled black ring maximal value of α' and the black string maximal value of α' agree.

KEYWORDS: Einstein-Gauss-Bonnet gravity, black rings, numerical solutions.

Contents

1. Introduction	2
2. The general formalism	3
2.1 The Einstein-Gauss-Bonnet theory	3
2.2 The Weyl solutions in $d = 5$ Einstein gravity and the rod structure	4
2.3 The static, axially symmetric Einstein-Gauss-Bonnet configurations	6
2.3.1 The equations	6
2.3.2 The rod structure	7
2.3.3 The physical quantities	9
2.3.4 Remarks on the free energy and thermodynamics	10
3. The known static solutions in $d = 5$ EGB theory	13
3.1 The Schwarzschild black hole in EGB theory	13
3.1.1 The solution in Schwarzschild coordinates	13
3.1.2 The solution in Weyl-type coordinates	14
3.2 The static uniform black string	16
4. The static EGB black rings	18
4.1 The static black rings in Einstein gravity	19
4.2 The static black rings in EGB theory	20
4.2.1 The ansatz and the physically relevant quantities	20
4.2.2 The numerical results	22
4.2.3 The large b limit and the maximal coupling $\alpha'_{s,\max}$	29
4.2.4 The phase diagram	33
5. Further remarks. Conclusions	34
A. The components of $G_{\mu\nu}$ and $H_{\mu\nu}$	36
B. Details on the numerics	38
B.1 A new coordinate system	38
B.2 The numerical methods	39
B.3 The issue of the maximal value of α'	41

1. Introduction

In recent years it has been realized that higher dimensions $d > 4$ allow for a rich landscape of black hole solutions that do not have four dimensional counterparts. The vacuum black ring solution of Emparan and Reall [1, 2] in $d = 5$ Einstein gravity is perhaps the best known example of such a configuration. The black ring has a horizon with topology $S^2 \times S^1$, while the Myers-Perry black hole [3] has a horizon topology S^3 . This solution provided also the first concrete piece of evidence that in higher dimensional gravity, the no-hair theorems of $3 + 1$ dimensions do not apply. For example, in a $4 + 1$ dimensional asymptotically flat spacetime with a given ADM mass and angular momentum, the geometry need not necessarily be that of the Myers-Perry black hole.

The $d = 5$ Emparan and Reall black ring solution has been generalized in various directions, including configurations with abelian matter fields [4]-[8]. Physically interesting solutions describing superposed black objects (black saturns [9], bicycling black rings [10], [11], and concentric rings [12], [13], [14]) were also constructed. However, in the static limit, all known $d = 5$ asymptotically flat solutions with a nonspherical horizon topology possess a conical singularity or other pathologies [2], [7], [8].

All these results concern the case of $d = 5$ Einstein gravity theory and its various extensions with abelian matter fields. However, in five dimensions, the most general theory of gravity leading to second order field equations for the metric is the so-called Einstein-Gauss-Bonnet (EGB) theory, which contains quadratic powers of the curvature. The Gauss-Bonnet (GB) term appears as the first curvature stringy correction to general relativity [15, 16], when assuming that the tension of a string is large as compared to the energy scale of other variables. Inclusion of this term in the action leads to a variety of new features (see [17], [18] for a review of the higher order gravity theories).

Although the generalization of the spherically symmetric Schwarzschild solution in EGB theory has been known for quite a long time [19], the issue of axially symmetric solutions with a GB term is basically unexplored. In particular we do not know if the $d \geq 5$ black holes with a nonspherical topology of the horizon continue to exist when including stringy correction to the action. The main obstacle here seems to be that the Weyl formalism, which has proven so useful in the case of Einstein gravity, allowing for the discovery of a plethora of interesting exact solutions, has no straightforward extension in the presence of a GB term.

In the absence of exact solutions, a natural way to approach this issue is to construct such configurations numerically. This paper aims at a first step in this direction, since we propose a framework for a special class of $d = 5$ static configurations with three commuting Killing vectors. In the absence of a GB term, this framework reduces to that used in [2] to construct generalized Weyl solutions. Here we argue that some basic properties there are still valid in the presence of a GB term, in particular the rod structure of the solutions.

As the simplest example of a $d = 5$ black object with a nonstandard topology of the event horizon, we present numerical evidence for the existence of static black rings in EGB theory. These solutions are found within a nonperturbative approach, by directly solving the second order field equations with suitable boundary conditions. These black rings

share most of the features of the Einstein gravity solution in [2]. Although the inclusion of the GB term in the action reduces the conical excess, these configurations still possess an angular deficit. Moreover, for a given value of the mass, similar to the case of a $d = 5$ EGB black string [20], the static black ring solutions exist up to a maximal value of the GB coupling constant.

The plan of the paper is the following. In the next Section we present a brief review of the Weyl formalism in Einstein gravity and argue that the coordinate system and the rod structure used there can be employed to construct EGB solutions as well. Section 3 consists of a discussion of the Schwarzschild black hole and the uniform black string in EGB theory. There we present evidence that these configurations can also be viewed as generalized Weyl solutions within the framework of Section 2. Section 4 contains the main results of this work consisting of a systematic study of the static black rings in EGB theory. We give our conclusions and remarks in the final section. There we report also our results on charged generalizations of the static black rings present in EGB-Maxwell theory. In Appendix A we present some details on the EGB equations. Appendix B contains a discussion of some technical aspects involved in the numerical construction of the EGB static black rings. This includes a new coordinate system which has proven more suitable for the numerical study of the black ring solutions.

2. The general formalism

2.1 The Einstein-Gauss-Bonnet theory

We consider the EGB action in five space-time dimensions

$$I = \frac{1}{16\pi G} \int_{\mathcal{M}} d^5x \sqrt{-g} [R + \alpha' L_{\text{GB}}] , \quad (2.1)$$

where G is the five dimensional Newton constant and α' is the GB coefficient with dimension $(length)^2$. In string theory, the GB coefficient is positive, and this is the only case considered in this work¹. R denotes the Ricci scalar and

$$L_{\text{GB}} = R^2 - 4R_{\mu\nu}R^{\mu\nu} + R_{\mu\nu\rho\sigma}R^{\mu\nu\rho\sigma} \quad (2.2)$$

the Gauss-Bonnet term with Ricci tensor $R_{\mu\nu}$ and Riemann tensor $R_{\mu\nu\rho\sigma}$.

The variation of the action (2.1) with respect to the metric tensor yields the EGB equations

$$E_{\mu\nu} = G_{\mu\nu} + \alpha' H_{\mu\nu} = 0 , \quad (2.3)$$

where

$$G_{\mu\nu} = R_{\mu\nu} - \frac{1}{2}g_{\mu\nu}R ,$$

$$H_{\mu\nu} = 2 \left[RR_{\mu\nu} - 2R_{\mu\rho}R_{\nu}^{\rho} - 2R_{\mu\rho\nu\sigma}R^{\rho\sigma} + R_{\mu\rho\sigma\lambda}R_{\nu}^{\rho\sigma\lambda} \right] - \frac{1}{2}g_{\mu\nu}L_{\text{GB}}.$$

¹Also, a negative value of α' leads to a number of pathological features of the theory, see *e.g.* [17].

For a well-defined variational principle, one has to supplement the action (2.1) with the Gibbons-Hawking surface term [21]

$$I_b^{(E)} = -\frac{1}{8\pi G} \int_{\partial\mathcal{M}} d^4x \sqrt{-\gamma} K, \quad (2.4)$$

and its counterpart for Gauss-Bonnet gravity [16]

$$I_b^{(GB)} = -\frac{\alpha'}{4\pi G} \int_{\partial\mathcal{M}} d^4x \sqrt{-\gamma} \left(J - 2G_{ab}K^{ab} \right), \quad (2.5)$$

where γ_{ab} is the induced metric on the boundary, K is the trace of the extrinsic curvature of the boundary, G_{ab} is the Einstein tensor of the metric γ_{ab} and J is the trace of the tensor

$$J_{ab} = \frac{1}{3}(2KK_{ac}K_b^c + K_{cd}K^{cd}K_{ab} - 2K_{ac}K^{cd}K_{db} - K^2K_{ab}). \quad (2.6)$$

2.2 The Weyl solutions in $d = 5$ Einstein gravity and the rod structure

Following the approach in [2], we consider asymptotically flat, five-dimensional static and axisymmetric vacuum spacetimes with three commuting Killing vector fields $V_{(i)}$ ($i = 1, 2, 3$). The commutativity of Killing vectors $[V_{(i)}, V_{(j)}] = 0$ enables us to find a coordinate system such that $V_{(i)} = \partial/\partial x^i$ and the metric is independent of the coordinates x^i . In what follows, we shall put $x^1 = t$, $x^2 = \psi$, and $x^3 = \varphi$. Then $(\partial/\partial x^1)$ is the Killing vector field associated with time translation and $(\partial/\partial x^2), (\partial/\partial x^3)$ denote the spacelike Killing vector fields with closed orbits.

Here we invoke the particularization for $d = 5$ of the general theorem 2.1 in Ref. [2]:

Let $V_{(i)}, i = 1, 2, 3$, be three-commuting Killing vector fields such that

1. $V_{(1)}^{[\mu_1} V_{(2)}^{\mu_2} V_{(3)}^{\mu_3} D^\nu V_{(i)}^{\rho]} = 0$ holds at least at one point of the spacetime for a given $i = 1, 2, 3$.
2. $V_{(i)}^\nu R_{\nu}^{[\rho} V_{(1)}^{\mu_1} V_{(2)}^{\mu_2} V_{(3)}^{\mu_3]} = 0$ holds for all $i = 1, 2, 3$.

Then the two-planes orthogonal to the Killing vector fields $V_{(i)}, i = 1, 2, 3$, are integrable.

The first condition holds because we have assumed axisymmetry, while the second one is automatically satisfied as long as we restrict ourselves to the vacuum solutions of Einstein equations.

As a result, the metric can be written in the canonical form [22] as

$$ds^2 = e^{2\nu(\rho, z)}(d\rho^2 + dz^2) + e^{2U_2(\rho, z)}d\psi^2 + e^{2U_3(\rho, z)}d\varphi^2 - e^{2U_1(\rho, z)}dt^2, \quad (2.7)$$

where $0 \leq \rho < \infty$, $-\infty < z < \infty$. Here it is most convenient to choose the three functions U_i as to satisfy the condition

$$\sum_i U_i = \log \rho. \quad (2.8)$$

This is compatible with the vacuum Einstein equations $G_{ij} = 0$ ($i = 1, 2, 3$), which for the choice (2.8) reduce to

$$\frac{\partial^2 U_i}{\partial \rho^2} + \frac{1}{\rho} \frac{\partial U_i}{\partial \rho} + \frac{\partial^2 U_i}{\partial z^2} = 0, \quad (2.9)$$

(the Einstein tensor for the metric ansatz (2.7) is presented in Appendix A). One can see that (2.9) is just Laplace's equation in a (fictitious) three-dimensional flat space with metric $ds^2 = d\rho^2 + \rho^2 d\theta^2 + dz^2$.

From the other components of the Einstein equations $G_\rho^\rho - G_z^z = 0$ and $G_\rho^z = 0$, we obtain the equations which determine the function $\nu(\rho, z)$ for a given solution of the equation (2.9)

$$\nu' = -\frac{1}{2\rho} + \frac{\rho}{2} \left(U_1'^2 + U_2'^2 + U_3'^2 - \dot{U}_1^2 - \dot{U}_2^2 - \dot{U}_3^2 \right), \quad \dot{\nu} = \rho(\dot{U}_1' + \dot{U}_2' + \dot{U}_3'), \quad (2.10)$$

where a prime denotes the derivative with respect to ρ and a dot denotes the derivative with respect to z . Solutions with the ansatz (2.7) and with U_1, U_2, U_3 and ν satisfying the equations (2.9), (2.10) are usually called generalized Weyl solutions.

Although the Einstein equations take a simple form in terms of (U_i, ν) , for the purposes of this paper it is more convenient to work with a set a functions f_i defined as follows

$$e^{2\nu(\rho, z)} = f_1(\rho, z), \quad e^{2U_2(\rho, z)} = f_2(\rho, z), \quad e^{2U_3(\rho, z)} = f_3(\rho, z), \quad e^{2U_1(\rho, z)} = f_0(\rho, z). \quad (2.11)$$

This leads to a line element

$$ds^2 = -f_0(\rho, z)dt^2 + f_1(\rho, z)(d\rho^2 + dz^2) + f_2(\rho, z)d\psi^2 + f_3(\rho, z)d\varphi^2, \quad (2.12)$$

which was used in our study of the EGB static black ring solutions.

In this paper we are mainly interested in configurations approaching asymptotically the five dimensional Minkowski spacetime, this being also the simplest solution of the equations (2.9), (2.10). In this case, the metric functions f_i have the following expression:

$$f_0(\rho, z) = 1, \quad f_1(\rho, z) = \frac{1}{2\sqrt{\rho^2 + z^2}}, \quad f_2(\rho, z) = \sqrt{\rho^2 + z^2} + z, \quad f_3(\rho, z) = \sqrt{\rho^2 + z^2} - z. \quad (2.13)$$

The usual form of the flat spacetime metric in the Hopf coordinates

$$ds^2 = -dt^2 + dr^2 + r^2(d\theta^2 + \cos^2 \theta d\psi^2 + \sin^2 \theta d\varphi^2), \quad (2.14)$$

is found from (2.12), (2.13) via the coordinate transformation

$$\rho = \frac{1}{2}r^2 \sin 2\theta, \quad z = \frac{1}{2}r^2 \cos 2\theta, \quad (2.15)$$

with $0 \leq r < \infty$, $0 \leq \theta \leq \pi/2$.

The equations (2.9), (2.10) possess a variety of physically interesting solutions. They can be uniquely characterized by the boundary conditions on the z -axis, known as the *rod-structure* [2], [22], [23]. In pure Einstein gravity, the physically relevant solutions for U_i can also be thought of as Newtonian potentials produced by thin rods of zero thickness with linear mass density $1/2$, placed on the axis of symmetry in the auxiliary three-dimensional flat space. Then the constraint (2.8) states that these sources must add up to give an infinite rod.

In this approach, the z -axis is divided into N intervals (called rods of the solution), $[-\infty, z_1], [z_1, z_2], \dots, [z_{N-1}, \infty]$. As proven in [22], in order to avoid curvature naked singularities at $\rho = 0$, it is a necessary condition that only one of the functions $f_0(0, z)$, $f_2(0, z)$, $f_3(0, z)$ becomes zero for a given rod, except for isolated points between the intervals.

For the static case discussed here, a horizon corresponds to a timelike rod where $f_0(0, z) = 0$ while $\lim_{\rho \rightarrow 0} f_0(\rho, z)/\rho^2 > 0$. There are also spacelike rods corresponding to compact directions specified by the conditions $f_a(0, z) = 0$, $\lim_{\rho \rightarrow 0} f_a(\rho, z)/\rho^2 > 0$, with $a = 2, 3$. A semi-infinite spacelike rod corresponds to an axis of rotation, the associated coordinate being a rotation angle. For example, the Minkowski spacetime (2.14) corresponds to two semi-infinite rods $[-\infty, 0]$ and $[0, \infty]$. Demanding regularity of the solutions at $\rho = 0$ imposes a periodicity 2π for both ψ and φ . (However, when several ψ - or φ -rods are present, it may be impossible to satisfy simultaneously all the periodicity conditions).

One of the main advantages of this approach is that the topology of the horizon is automatically imposed by the rod structure. This provides a simple way to construct a variety of solutions with nontrivial topology of the horizon (including multi-black objects). Since (2.9) is linear, one can superpose different solutions for the same potential U_i . The nonlinear nature of the Einstein gravity manifests itself through the equation (2.10) for the metric function ν .

2.3 The static, axially symmetric Einstein-Gauss-Bonnet configurations

2.3.1 The equations

One of the main purposes of this work is argue that the ansatz (2.7) and the associated rod structure can be used to construct physically relevant solutions in EGB theory. *A priori*, it is not clear that this metric ansatz is valid also in this case, since the second assumption in the general theorem mentioned above (*i.e.* $V_{(i)}^\nu R_{\nu}^{\mu_1} V_{(1)}^{\mu_2} V_{(2)}^{\mu_3} = 0$) does not hold in general for EGB theory. Thus the situation here is similar to the case of caged black holes [24], [25] or nonuniform black strings [26], [27] in Kaluza-Klein Einstein gravity, where the validity of the metric ansatz could be proven only *a posteriori*, after solving the field equations.

The equations for the functions f_1 , f_2 , f_3 and f_0 are found by using a suitable combination of the EGB equations, $E_t^t = 0$, $E_\rho^\rho + E_z^z = 0$, $E_\psi^\psi = 0$, and $E_\varphi^\varphi = 0$. Details on these equations and the explicit form of the tensors G_μ^ν and H_μ^ν are presented in Appendix A.

The remaining equations $E_z^\rho = 0$, $E_\rho^\rho - E_z^z = 0$ yield two constraints. Following [26], we note that setting $E_t^t = E_\varphi^\varphi = E_\rho^\rho + E_z^z = 0$ in $\nabla_\mu E^{\mu\rho} = 0$ and $\nabla_\mu E^{\mu z} = 0$, we obtain the Cauchy-Riemann relations

$$\partial_\rho (\sqrt{-g} E_z^\rho) + \partial_\rho \left(\sqrt{-g} \frac{1}{2} (E_\rho^\rho - E_z^z) \right) = 0, \quad \partial_\rho (\sqrt{-g} E_z^\rho) - \partial_z \left(\sqrt{-g} \frac{1}{2} (E_\rho^\rho - E_z^z) \right) = 0. \quad (2.16)$$

Thus the weighted constraints satisfy Laplace equations, and the constraints are fulfilled, when one of them is satisfied on the boundary and the other at a single point [26].

Due to the GB contributions, the second order equations for the functions f_i are much more complicated than in the case of Einstein gravity and do not reduce to the simple Laplace equation. Thus the functions U_i are no longer harmonic. Also, one can verify

that the central property (2.8) of the Einstein gravity Weyl-solutions does not hold in the presence of a GB term and thus one cannot set $f_0 f_2 f_3 = \rho^2$.

Therefore finding closed form solutions within this approach looks unlikely. However, the solutions can be constructed numerically, by solving boundary value problems. A major advantage of the ansatz (2.7) is that the (ρ, z) coordinates have a rectangular boundary in which all boundaries coincide with the coordinate lines and thus are suitable for numerics².

2.3.2 The rod structure

The central point in this approach is that the rod structure, as explained above for the case of Einstein gravity, can be used also for solutions of the EGB theory³. This would fix the boundary conditions along the z -axis for the functions f_i and thus the topology of the horizon.

Here one starts by noticing that the following generic form of a solution near the z -axis is compatible with the EGB equations:

$$f_i(\rho, z) = f_{i0}(z) + \rho^2 f_{i2}(z) + \dots, \quad (2.17)$$

where the functions $f_{ik}(z)$ are solutions of a complicated set of nonlinear second order ordinary differential equations. Then, similar to the case of Einstein gravity, the z -axis is divided into N intervals—the rods of the solution. Except for isolated points between the rods, one assumes that only one of the functions $f_0(0, z)$, $f_2(0, z)$, $f_3(0, z)$ becomes zero for a given rod, while the remaining functions stay finite at $\rho = 0$ in general. (In fact, if more than one of these functions is going to zero for a given z inside a rod, one can prove following the arguments in [22], that there is a curvature singularity at that point.) Again, one imposes the condition that the N intervals must add up to give an infinite rod.

For example, for a rod in the ψ -direction, one finds the following expansion of the metric functions as $\rho \rightarrow 0$:

$$\begin{aligned} f_0(\rho, z) &= f_{20}(z) + \rho^2 f_{22}(z) + \dots, & f_1(\rho, z) &= f_{10}(z) + \rho^2 f_{12}(z) + \dots, \\ f_2(\rho, z) &= \rho^2 f_{22}(z) + \rho^4 f_{24}(z) + \dots, & f_3(\rho, z) &= f_{30}(z) + \rho^2 f_{32}(z) + \dots \end{aligned} \quad (2.18)$$

The important feature here is that the constraint equation $E_\rho^z = 0$ implies $f_{10}(z)/f_{22}(z) = c_1$, *i.e.* a well-defined periodicity for the coordinate ψ .

Therefore, in order to cure the conical singularity at the rod, the coordinate ψ should have a periodicity $\Delta\psi = 2\pi\sqrt{c_1}$. A different periodicity of ψ implies the occurrence of a conical singularity (this is the case if there are several different ψ -rods).

Similar results holds also for a rod in the φ -direction (*i.e.* when interchanging f_2 and f_3), the periodicity of φ there being again fixed by the constraint equation $E_\rho^z = 0$, *i.e.* $\lim_{\rho \rightarrow 0} \rho^2 f_1/f_3 = c_2$.

²This is not the case of the ring coordinates used in most of the studies on black ring solutions. The spatial infinity corresponds there to a single point.

³However, note that the interpretation of a rod as corresponding to a zero thickness source with linear mass density 1/2, placed on the axis of symmetry in a auxiliary three-dimensional flat space is no longer valid in EGB theory.

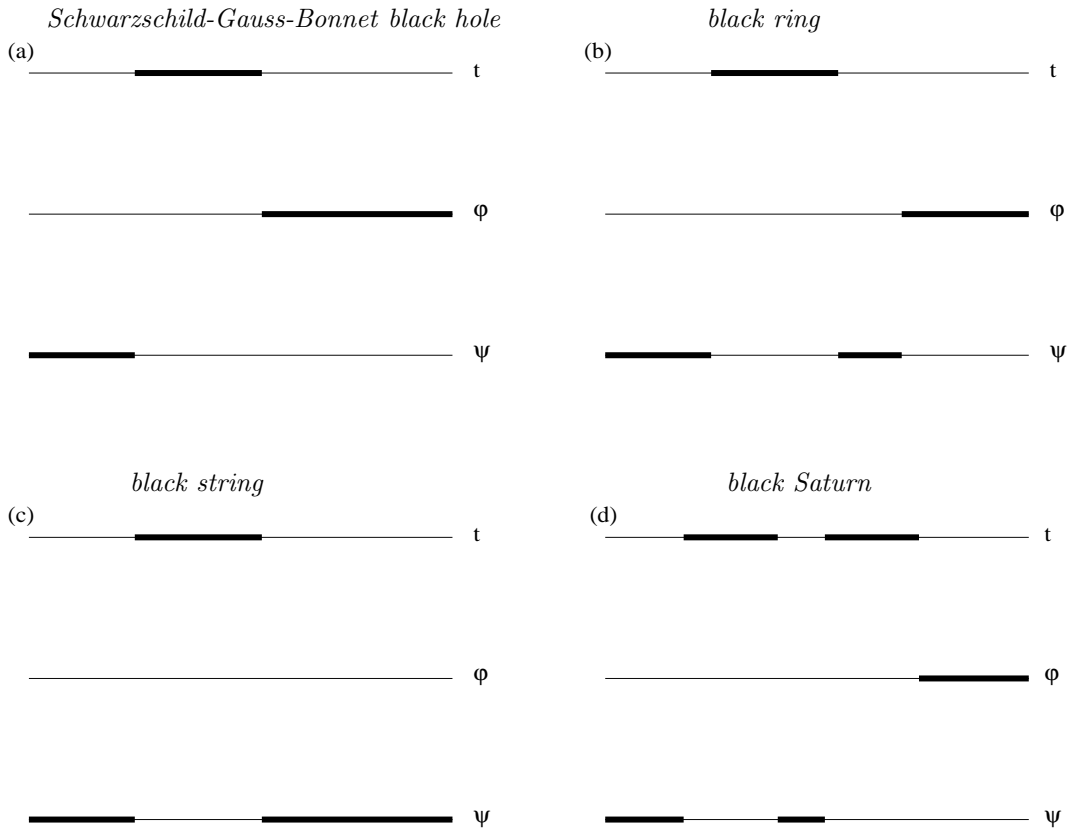


Figure 1. The rod structure of the solutions is shown for several EGB solutions. The thin lines denote the z -axis and the thick lines denote the rods.

A finite timelike rod corresponds to an event horizon, where⁴

$$\begin{aligned}
 f_0(\rho, z) &= \rho^2 f_{02}(z) + \rho^4 f_{04}(z) + \dots, & f_1(\rho, z) &= f_{10}(z) + \rho^2 f_{12}(z) + \dots, \\
 f_2(\rho, z) &= f_{20}(z) + \rho^2 f_{22}(z) + \dots, & f_3(\rho, z) &= f_{30}(z) + \rho^2 f_{32}(z) + \dots,
 \end{aligned}
 \tag{2.19}$$

with $\lim_{\rho \rightarrow 0} \rho^2 f_1/f_0 = c_3$, which fixes the Hawking temperature of solutions.

Thus, depending on the physical situation we consider, the boundary conditions along the z -axis are fixed by the above relations. The obvious boundary conditions for large ρ, z is that the functions f_i approach the Minkowski background functions (2.13).

Similar to the case of Einstein gravity, the topology of the horizon is fixed by the boundary conditions satisfied by f_2 and f_3 at the ends of the corresponding (finite) timelike rod⁵.

For example, if either end of this rod continues with rods of different angular directions, then the event horizon has an S^3 topology (see Figure 1a). A black ring corresponds to f_2 or f_3 vanishing at both ends of the finite timelike rod associated with the horizon (see Figure 1b). One can consider as well a black Saturn combining both types of black objects

⁴ $f_{ik}(z)$ here should not be confused with those in (2.18).

⁵A timelike rod extending to infinity corresponds to an acceleration horizon.

above, with two different horizons (see Figure 1d). Moreover, if both ψ - and φ -rods extend to infinity, then the spacetime is asymptotically flat. Solutions in Kaluza-Klein theory (for example a black string without a rod on the ψ - or ϕ -direction (see Figure 1c)) can also be considered.

It is tempting to conjecture that, similar to the case of Einstein gravity [23], a $d = 5$ EGB solution within the ansatz (2.12), is uniquely specified by its rod structure.

2.3.3 The physical quantities

The general results in the literature [28] show that, similar to the case of Einstein gravity, the mass M of an asymptotically flat EGB solution can be read from the asymptotic expression for the metric component g_{tt}

$$-g_{tt} = f_0 \sim 1 - \frac{4GM}{3\pi\sqrt{\rho^2 + z^2}} + \dots \quad (2.20)$$

Supposing we have an event horizon for $z_1 \leq z \leq z_2$, the horizon metric is given by⁶

$$d\sigma^2 = f_1(0, z)dz^2 + f_2(0, z)d\psi^2 + f_3(0, z)d\varphi^2. \quad (2.21)$$

Two quantities associated with the event horizon are the event horizon area A_H and the Hawking temperature. For the metric ansatz (2.12) these are given by

$$A_H = \Delta\psi\Delta\varphi \int_{z_1}^{z_2} dz \sqrt{f_1(0, z)f_2(0, z)f_3(0, z)}, \quad T_H = \frac{1}{2\pi} \lim_{\rho \rightarrow 0} \sqrt{\frac{f_0(\rho, z)}{\rho^2 f_1(\rho, z)}}. \quad (2.22)$$

For solutions in EGB theory it is also of interest to compute the Ricci scalar of the horizon

$$R_{\Sigma_h} = \frac{1}{2f_1(0, z)} \left(\frac{\dot{f}_1(0, z)\dot{f}_2(0, z)}{f_1(0, z)f_2(0, z)} + \frac{\dot{f}_1(0, z)\dot{f}_3(0, z)}{f_1(0, z)f_3(0, z)} - \frac{\dot{f}_2(0, z)\dot{f}_3(0, z)}{f_2(0, z)f_3(0, z)} + \frac{\dot{f}_2^2(0, z)}{f_2^2(0, z)} + \frac{\dot{f}_3^2(0, z)}{f_3^2(0, z)} - 2\left(\frac{\dot{f}_2(0, z)}{f_2(0, z)} + \frac{\dot{f}_3(0, z)}{f_3(0, z)}\right) \right). \quad (2.23)$$

Considering now the case of a space-like ψ -rod for $z_3 \leq z \leq z_4$, one writes the line element on this three-dimensional surface Σ_δ

$$d\sigma^2 = f_1(0, z)dz^2 + f_3(0, z)d\varphi^2 - f_0(0, z)dt^2. \quad (2.24)$$

The first quantity of interest is the proper length of the rod

$$L = \int_{z_3}^{z_4} dz \sqrt{f_1(0, z)}, \quad (2.25)$$

(note that for a finite rod, L differs from the coordinate distance $\Delta z = z_4 - z_3$).

The solutions we are interested in may possess a conical singularity along some region of the symmetry axis. To define a conical singularity for a rotational axis with angle ψ one computes the proper circumference C around the axis and its proper radius R and defines:

$$\alpha = \frac{dC}{dR} \Big|_{R=0} = \lim_{\rho \rightarrow 0} \frac{\sqrt{g_{\psi\psi}}\Delta\psi}{\int_0^\rho \sqrt{g_{\rho\rho}}d\rho} = \lim_{\rho \rightarrow 0} \frac{\partial_\rho \sqrt{g_{\psi\psi}}\Delta\psi}{\sqrt{g_{\rho\rho}}}, \quad (2.26)$$

⁶If there are several horizons, then one should write such an expansion for each of them.

where $\Delta\psi$ is the period of ψ . The presence of a conical singularity is now expressed⁷ by means of:

$$\delta = 2\pi - \alpha = 2\pi \left(1 - \lim_{\rho \rightarrow 0} \sqrt{\frac{f_2(\rho, z)}{\rho^2 f_1(\rho, z)}} \right), \quad (2.27)$$

such that $\delta > 0$ corresponds to a conical deficit, while $\delta < 0$ corresponds to a conical excess. A conical deficit can be interpreted as a string stretched along on a certain segment of the z -axis, while a conical excess is a strut pushing apart the rods connected to that segment (in fact, for $d = 5$, the struts and strings are two dimensional surfaces). Similar to Einstein gravity, a constant rescalings of ψ can be used to eliminate possible conical singularities on a given segment, but in general, once this is fixed, there will remain conical singularities at other ψ -segments.

For $\delta < 0$, we have found it convenient to introduce the quantity

$$\bar{\delta} = \frac{\delta/(2\pi)}{1 - \delta/(2\pi)}, \quad (2.28)$$

which has a finite range and measures the 'relative angular excess'.

Of interest here is to compute the spacetime area spanned by the ψ -rod. This is done by going to the Euclidean section $t \rightarrow i\tau$ and evaluating the quantity

$$Area = \beta \Delta\varphi \int_{z_3}^{z_4} dz \sqrt{f_0(0, z) f_1(0, z) f_3(0, z)}, \quad (2.29)$$

where $\beta = 1/T_H$ is the periodicity of the Euclidean time. For completeness, we give here also the expression for the Ricci scalar on the ψ -rod,

$$R_{\Sigma_\delta} = \frac{1}{2f_1(0, z)} \left(\frac{\dot{f}_1(0, z)\dot{f}_0(0, z)}{f_1(0, z)f_0(0, z)} + \frac{\dot{f}_1(0, z)\dot{f}_3(0, z)}{f_1(0, z)f_3(0, z)} - \frac{\dot{f}_0(0, z)\dot{f}_3(0, z)}{f_0(0, z)f_3(0, z)} + \frac{\dot{f}_0^2(0, z)}{f_0^2(0, z)} + \frac{\dot{f}_3^2(0, z)}{f_3^2(0, z)} - 2\left(\frac{\ddot{f}_0(0, z)}{f_0(0, z)} + \frac{\ddot{f}_3(0, z)}{f_3(0, z)}\right) \right). \quad (2.30)$$

Of course, similar expressions can be written when considering instead a φ -rod.

2.3.4 Remarks on the free energy and thermodynamics

The discussion in this subsection applies to asymptotically flat solutions (although it can easily be generalized to the Kaluza-Klein case).

The gravitational thermodynamics of the EGB black objects can be formulated via the path integral approach [21, 29]. In what follows it is important to use the observation that one can write

$$R_t^t \sqrt{-g} = -\frac{1}{2} \left(\partial_\rho \left(\sqrt{\frac{f_2 f_3}{f_0}} f'_0 \right) + \partial_z \left(\sqrt{\frac{f_2 f_3}{f_0}} \dot{f}_0 \right) \right), \quad (2.31)$$

$$\left(H_t^t + \frac{1}{2} L_{GB} \right) \sqrt{-g} = \frac{1}{2} (\partial_\rho T_\rho + \partial_z T_z), \quad (2.32)$$

⁷Note that, in some sense, fixing δ is the analogue of computing the Hawking temperature on the Euclidean section.

where

$$\begin{aligned}
T_\rho = & \sqrt{\frac{f_2 f_3}{f_0}} \left(\frac{f'_0}{f_1} \left(\frac{\dot{f}_2 \dot{f}'_3}{f_2 f_3} - \frac{\dot{f}_2 \dot{f}_3}{f_2 f_3} \right) + \frac{\dot{f}_0}{f_1} \left(\frac{\dot{f}_2 \dot{f}'_0}{f_0 f_2} + \frac{\dot{f}_3 \dot{f}'_0}{f_0 f_3} + \frac{\dot{f}_2 \dot{f}'_3}{f_2 f_3} + \frac{\dot{f}_3 \dot{f}'_2}{f_2 f_3} \right) + \frac{f'_0}{f_1^2 f_2} (f'_1 f'_2 + \dot{f}_1 \dot{f}_2) \right. \\
& + \frac{\dot{f}_0}{f_1^2 f_2} (\dot{f}_2 \dot{f}'_1 - \dot{f}_1 \dot{f}'_2) + \frac{\dot{f}_0}{f_1^2 f_3} (\dot{f}_3 \dot{f}'_1 - \dot{f}_1 \dot{f}'_3) + \frac{f'_0}{f_1^2 f_3} (f'_1 f'_3 + \dot{f}_1 \dot{f}_3) \\
& \left. - \frac{\dot{f}_0^2}{f_0 f_1} \left(\frac{\dot{f}_3}{f_3} + \frac{\dot{f}_2}{f_2} \right) - \frac{2\dot{f}'_0}{f_1} \left(\frac{\dot{f}_2}{f_2} + \frac{\dot{f}_3}{f_3} \right) + \frac{2\ddot{f}_0}{f_1} \left(\frac{\dot{f}_2}{f_2} + \frac{\dot{f}_3}{f_3} \right) \right), \tag{2.33} \\
T_z = & \sqrt{\frac{f_2 f_3}{f_0}} \left(\frac{f'_0}{f_1 f_2 f_3} (\dot{f}_2 \dot{f}'_3 + \dot{f}_3 \dot{f}'_2) + \frac{\dot{f}_0}{f_1 f_2 f_3} (\dot{f}_2 \dot{f}_3 - f'_2 f'_3) + \frac{\dot{f}_0 f'_0}{f_0 f_1} \left(\frac{\dot{f}_3}{f_3} + \frac{\dot{f}_2}{f_2} \right) \right. \\
& - \frac{f_0^2}{f_0 f_1} \left(\frac{\dot{f}_2}{f_2} + \frac{\dot{f}_3}{f_3} \right) + \frac{f'_0}{f_1^2 f_2} (\dot{f}_1 \dot{f}'_2 - \dot{f}_2 \dot{f}'_1) + \frac{\dot{f}_0}{f_1^2 f_2} (f'_1 f'_2 + \dot{f}_1 \dot{f}_2) \\
& \left. + \frac{f'_0}{f_1^2 f_3} (\dot{f}_1 \dot{f}'_3 - \dot{f}_3 \dot{f}'_1) + \frac{\dot{f}_0}{f_1^2 f_3} (f'_1 f'_3 + \dot{f}_1 \dot{f}_3) - \frac{2\dot{f}'_0}{f_1} \left(\frac{\dot{f}_2}{f_2} + \frac{\dot{f}_3}{f_3} \right) + \frac{2f''_0}{f_0} \left(\frac{\dot{f}_2}{f_2} + \frac{\dot{f}_3}{f_3} \right) \right).
\end{aligned}$$

When computing the classical bulk action evaluated on the equations of motion, one replaces the $R + \alpha' L_{GB}$ volume term with $2(R_t^t + \alpha'(H_t^t + L_{GB}/2))$ and make use of (2.31) to express it as a difference of two boundary integrals. The boundary integral at infinity should be evaluated together with the contributions from $I_b^{(E)}$ and $I_b^{(GB)}$. As usual, this quantity is divergent. To regularize it, one has to subtract the contribution of the Minkowski background for *both* Einstein and Gauss-Bonnet boundary terms⁸.

A direct computation implies the following expression for the tree level action of a single black object in $d = 5$ EGB theory (the extension to multi-black objects is straightforward)

$$I_0 = \beta(M - \frac{1}{4G} T_H(A_H + \alpha' A_1)), \tag{2.34}$$

with

$$A_1 = 2 \int_{\Sigma_h} d^3 x \sqrt{\tilde{h}} R_{\Sigma_h}, \tag{2.35}$$

where $\tilde{h} = \sqrt{f_1 f_2 f_3}$ is the determinant of the induced metric on the horizon and R_{Σ_h} is the event horizon curvature as given by (2.23).

The above results hold for the case of configurations with a regular z -axis (*i.e.* the periodicity of both angles ψ and φ is 2π everywhere). It is interesting to extend this analysis to the case of EGB solutions with conical singularities (this is the case of the black rings discussed in the Section 4). For simplicity, we shall consider here the case of a

⁸Note that for asymptotically flat solutions, the Gibbons-Hawking boundary term (2.4) gives a divergent contribution to I_0 , while the GB boundary term reduces to a constant factor. It would be interesting to generalize the quasilocal formalism and the renormalized boundary stress-tensor from Einstein gravity to EGB theory. This will avoid the requirement to choose a background for the solutions. For example, we have found that the usual counterterm used in [30] for the black rings in Einstein theory regularizes also the mass and action of some (asymptotically flat-) EGB solutions, including the black rings discussed in Section 4. However, this approach implies the existence of a constant term $\sim \beta\alpha'$ in the action, originating in the contribution of the GB boundary term (2.5).

single singular section of the z -axis associated with a ψ -rod (the generalization to other cases is straightforward). Then the conical singularity will add an extra contribution to the total tree level Euclidean action of the system, which leads to a more complicated thermodynamics of the system (see *e.g.* [31] for a related discussion for the $d = 4$ Israel-Kahn solution). This contribution can be evaluated by using the relations [32]

$$\frac{1}{2} \int_{\Sigma_\delta} d^5x \sqrt{g} R = Area \delta, \quad \frac{1}{2} \int_{\Sigma_\delta} d^5x \sqrt{g} L_{GB} = Area_1 \delta, \quad (2.36)$$

where $Area$ is the space-time area of the surface spanned by the conical singularity and

$$Area_1 = 2 \int_{\Sigma_\delta} d^3x \sqrt{\bar{h}} R_{\Sigma_\delta}, \quad (2.37)$$

with $\bar{h} = \sqrt{f_1 f_0 f_3}$ the determinant of the induced metric on the surface Σ_δ and R_{Σ_δ} the Ricci scalar on Σ_δ as given by (2.30).

Thus the total action in the presence of a conical singularity becomes

$$I = \beta \left(M - \frac{1}{4G} T_H (A_H + \alpha' A_1) \right) - \frac{1}{8\pi G} (Area + \alpha' Area_1) \delta. \quad (2.38)$$

The free energy of the solutions is identified as $F = T_H I = \mathcal{M} - T_H S$, where \mathcal{M} is the mass which enters the thermodynamics and S is the entropy. The entropy of the EGB black hole solutions *without* conical singularities can be written as an integral over the event horizon [33]:

$$S = \frac{1}{4G} \int_{\Sigma_h} d^3x \sqrt{\bar{h}} (1 + 2\alpha' R_{\Sigma_h}), \quad (2.39)$$

which is the sum of one quarter of the event horizon area plus a Gauss-Bonnet correction. In this case, the mass \mathcal{M} computed from the first law of thermodynamics is equal to the mass M computed at infinity.

It would be interesting to perform a similar computation for solutions with conical singularities. Similar to the case of Einstein gravity [34], a new extensive parameter $\mathcal{A} = (Area + \alpha' Area_1)/\beta$ associated with the rod containing the conical singularity will appear here, while the free energy becomes a function of both T_H and \mathcal{A} . Also, the first law of thermodynamics contains an extra-work term $\mathcal{T} d\mathcal{A}$ (with $\mathcal{T} = -\delta/8\pi G$ the tension associated with \mathcal{A}). Then the entropy S and the thermodynamical mass \mathcal{M} of the physical system are given by

$$S = - \left. \frac{\partial F}{\partial T_H} \right|_{\mathcal{A}}, \quad \mathcal{M} = F + T_H S. \quad (2.40)$$

The thermodynamical stability of the EGB solutions can be studied in the usual way. For example, one defines the specific heat of a black object $C = T_H \left(\frac{\partial S}{\partial T_H} \right)$, with $C > 0$ for thermodynamically stable solutions.

3. The known static solutions in $d = 5$ EGB theory

3.1 The Schwarzschild black hole in EGB theory

3.1.1 The solution in Schwarzschild coordinates

The black hole solutions of EGB gravity have been studied beginning with the work of [19] more than 20 years ago. Most of the solutions in the literature restricted to static, spherically symmetric configurations and a Schwarzschild coordinate system. A suitable metric ansatz in this case is

$$ds^2 = \frac{dr^2}{N(r)} + r^2(d\theta^2 + \sin^2\theta d\varphi^2 + \cos^2\theta d\psi^2) - N(r)\sigma^2(r)dt^2, \quad (3.1)$$

and the expressions for $N(r)$ and $\sigma(r)$ depend on the matter content of the theory.

The Hawking temperature of a generic black hole (3.1) is $T_H = N'(r_h)\sigma(r_h)/(4\pi)$, where a prime denotes the derivative with respect to the radial coordinate and r_h is the largest positive root of $N(r)$, typically associated to the outer horizon of a black hole. Also, the event horizon area of a black hole is $A_H = V_3 r_h^3$ (with $V_3 = 2\pi^2$ the area of the three-sphere).

The complexity of the EGB theory, basically due to higher order terms in the curvature tensor, makes the task of finding exact solutions very difficult. To the best of our knowledge, the only $d = 5$ static, spherically symmetric EGB solutions known in closed form are the generalizations of (electro-)vacuum Einstein gravity configurations⁹. The Schwarzschild black hole in EGB theory has $\sigma(r) = 1$, the metric function $N(r)$ being given by¹⁰

$$N(r) = 1 + \frac{r^2}{4\alpha'} \left(1 - \sqrt{1 + \frac{8\alpha'(r_h^2 + 2\alpha')}{r^4}} \right). \quad (3.2)$$

The constant r_h in (3.2) corresponds to the event horizon radius. One should note that the EGB Schwarzschild solution exists for all $r_h > 0$ and $\alpha' \geq 0$. As $r \rightarrow r_h$ one finds

$$N(r) = \frac{2r_h}{r_h^2 + 4\alpha'}(r - r_h) + O(r - r_h)^2. \quad (3.3)$$

At short distances, the EGB Schwarzschild solution and its Einstein gravity counterpart are substantially different due to the effect of the GB term. An interesting feature is that the EGB Schwarzschild metric turns out to be finite at the origin, since $N(r) \rightarrow 1 - \sqrt{(r_h^2 + 2\alpha')/(2\alpha')}$ as $r \rightarrow 0$. However, at large distances ($r^2 \gg \alpha'$) the EGB black hole behaves like the Schwarzschild solution. Once the event horizon radius r_h is fixed (as is done in the numerical construction of the solutions), the parameter α' enters the $1/r^2$ term in the asymptotics,

$$N(r) = 1 - \frac{r_h^2 + 2\alpha'^2}{r^2} + \frac{2\alpha'(r_h^2 + 2\alpha'^2)^2}{r^6} + O(1/r^{10}). \quad (3.4)$$

⁹Exact solutions describing cosmic strings in $d = 5$ EGB theory were found in [35]. Obviously, these solutions cannot be described within the metric ansatz (3.1).

¹⁰The usual form for $N(r)$ in the literature is in terms of $r_h^2 = m - 2\alpha'$, which corresponds to fixing the mass of the solutions. However, the expression (3.2) fits better with the purposes of this work.

Also, as $\alpha' \rightarrow 0$, one recovers to leading order the Schwarzschild black hole expression

$$N(r) = 1 - \frac{r_h^2}{r^2} + \left(-\frac{2}{r^2} + \frac{2r_h^4}{r^6}\right)\alpha' + O(\alpha')^2. \quad (3.5)$$

The Hawking temperature and the mass of these solutions are given by

$$T_H = \frac{r_h}{2\pi(r_h^2 + 4\alpha')}, \quad M = \frac{3V_3}{16\pi G}(r_h^2 + 2\alpha'). \quad (3.6)$$

The above expression for M shows the existence of a mass gap: black holes exist only for $M > 3V_3\alpha'/(8\pi G)$. Thus the mass spectrum of the spherically symmetric EGB black holes is bounded from below.

A straightforward computation leads to the following expression for the entropy of the EGB Schwarzschild black holes

$$S = S_0 + S_c \quad \text{with} \quad S_0 = \frac{A_H}{4G}, \quad S_c = 3\alpha' \frac{V_3 r_h}{G}. \quad (3.7)$$

One can easily verify that the first law of thermodynamics $dM = T_H dS$ also holds.

Without entering into details, we mention the existence of some substantial differences between the thermodynamics of the EGB Schwarzschild solutions and their Einstein gravity counterparts. If the black holes are large enough $r_h \gg \sqrt{\alpha'}$, then they behave like their Schwarzschild-Tangerlini counterparts. A different picture is found for small values of r_h , since $T_H \simeq r_h/(8\pi\alpha')$ in that case. Therefore, the specific heat changes its sign at length scales of order $r_h \sim \sqrt{\alpha'}$. This implies the existence of a branch of five dimensional EGB black holes which is thermodynamically stable (see the Ref. [17] for a review of these aspects).

3.1.2 The solution in Weyl-type coordinates

To bring the generic metric (3.1) to Weyl form (2.12), one considers the coordinate transformation

$$\rho = \frac{1}{2}r_0^2 \sinh G(r) \sin 2\theta, \quad z = \frac{1}{2}r_0^2 \cosh G(r) \cos 2\theta, \quad (3.8)$$

where r_0 is defined by the asymptotic expansion of $N(r) = 1 - (r_0/r)^2 + \dots$ (*i.e.* $r_0^2 = r_h^2 + 2\alpha'$). The function $G(r)$ above is defined as

$$G(r) = 2 \int_{r_h}^r \frac{dx}{x\sqrt{N(x)}} \quad (3.9)$$

(with $G(r_h) = 0$). Then the Schwarzschild coordinate r is expressed in terms of Weyl coordinates ρ, z as

$$r(\rho, z) = G^{-1}(\operatorname{arsinh} \sqrt{X(\rho, z)}), \quad (3.10)$$

where

$$X(\rho, z) = \frac{1}{2} \left(\frac{4}{r_0^2}(\rho^2 + z^2) + \sqrt{\frac{16\rho^2}{r_0^2} + \left(1 - \frac{4(\rho^2 + z^2)}{r_0^2}\right)^2} \right). \quad (3.11)$$

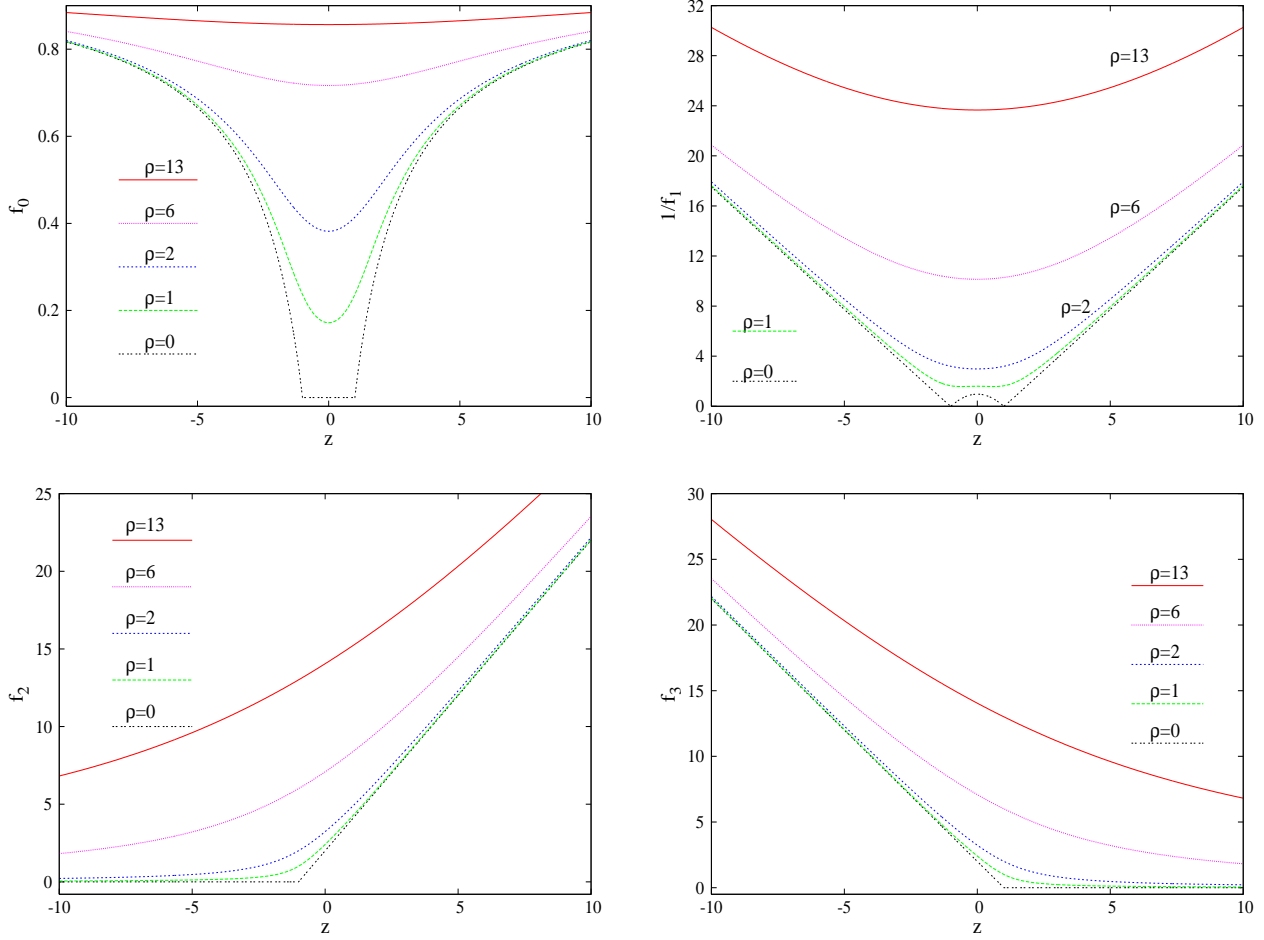


Figure 2. The metric functions f_i of an EGB Schwarzschild black hole are shown versus z for several values of ρ . The relevant parameters here are $a = 1$, $\alpha' = 0.01$.

A straightforward but cumbersome computation leads to the following expression for the metric functions for the parametrization (2.12)

$$\begin{aligned}
 f_0(\rho, z) &= F(r(\rho, z))\sigma^2(r(\rho, z)), & f_1(\rho, z) &= \frac{r(\rho, z)P^2(\rho, z)}{1 + P^4(\rho, z)}, \\
 f_2(\rho, z) &= \frac{1}{2}r^2(\rho, z)\left(1 + \frac{1}{\sqrt{P^2(\rho, z) + 1}}\right), & f_3(\rho, z) &= \frac{1}{2}r^2(\rho, z)\left(1 - \frac{1}{\sqrt{P^2(\rho, z) + 1}}\right),
 \end{aligned}
 \tag{3.12}$$

with

$$P(\rho, z) = \frac{\rho}{z} \sqrt{\frac{X(\rho, z) + 1}{X(\rho, z)}}.
 \tag{3.13}$$

Unfortunately, the integral (3.9) cannot be computed in closed form for the known solutions of EGB theory (except for the asymptotic expressions as $r \rightarrow r_h$ and $r \rightarrow \infty$). However, the expressions (3.9), (3.12) can be evaluated numerically.

For any value of α' , the rod structure of the EGB Schwarzschild black hole as resulting from (3.12) consists of a semi-infinite space-like rod $[-\infty, -a]$ (with $f_2(0, z) = 0$ there), a finite time-like rod $[-a, a]$ ($f_0(0, z) = 0$) and a semi-infinite space-like rod $[a, \infty]$ (with vanishing $f_3(0, z)$) in the φ -direction (with $a = r_0^2/4$). Thus the topology of the horizon is S^3 as required (see Figure 1a). A plot of the metric functions f_i exhibiting this rod structure for a typical EGB Schwarzschild solution is shown in Figure 2. In principle, most of the physically relevant properties of the EGB Schwarzschild black hole can also be rederived within the metric ansatz (2.12). However, the required computation is much more difficult for that coordinate system.

3.2 The static uniform black string

It is of interest to briefly review the situation for a different type of black object in EGB theory which can also be studied within the ansatz (2.12). In Einstein gravity, one can construct uniform $d = 5$ black string solutions by adding a flat direction to any $d = 4$ vacuum black hole. (These solutions can still be written in the $d = 5$ Weyl form (2.12), the new direction ψ being trivial.) However, it is straightforward to check that this simple construction does not work in the presence of a GB term in the action¹¹, unless the solutions are conformally flat. Although no exact solutions describing $d = 5$ black strings in EGB theory are known so far, these configurations were studied numerically in Ref. [20]. These solutions can be constructed within a metric ansatz related to (3.1)

$$ds^2 = \frac{dr^2}{N(r)} + r^2(d\theta^2 + \sin^2\theta d\psi^2) - N(r)\sigma^2(r)dt^2 + b(r)d\varphi^2, \quad (3.14)$$

(note that $0 \leq \theta \leq \pi$ in this case while the periodicity of φ is not fixed *a priori*). The new feature here as compared to the case of Einstein gravity is that the metric component $g_{\varphi\varphi}$ differs from one.

The event horizon of a uniform black string is located at $r = r_h > 0$, where the following approximate form of the metric functions holds

$$\begin{aligned} N(r) &= N_1(r - r_h) + O(r - r_h)^2, \quad \sigma(r) = \sigma_h + \sigma_1(r - r_h) + O(r - r_h)^2, \\ b(r) &= b_h + b_1(r - r_h) + O(r - r_h)^2, \end{aligned} \quad (3.15)$$

where

$$\begin{aligned} b_1 &= \frac{2b_h(r_h - N_1 r_h^2 + 4N_1\alpha' + 2N_1^2 r_h \alpha')}{N_1(r_h^2 + 4\alpha')(2N_1\alpha' - r_h)}, \\ \sigma_1 &= \sigma_h \left(-r_h^2(-1 + N_1 r_h)(1 + 6N_1 r_h) + 2N_1 r_h(4 + 3N_1 r_h(3 + 4N_1 r_h))\alpha' \right. \\ &\quad \left. - 8N_1^2(1 + 3N_1 r_h(-3 + N_1 r_h))\alpha'^2 - 112N_1^4\alpha'^3 \right) \left(6N_1^2 r_h(r_h^2 + 4\alpha')(-2\alpha' + (r_h - 2N_1\alpha')^2) \right)^{-1}, \end{aligned} \quad (3.16)$$

while

$$N_1 = \frac{r_h - \sqrt{r_h^2 - 8\alpha'}}{4\alpha'}. \quad (3.17)$$

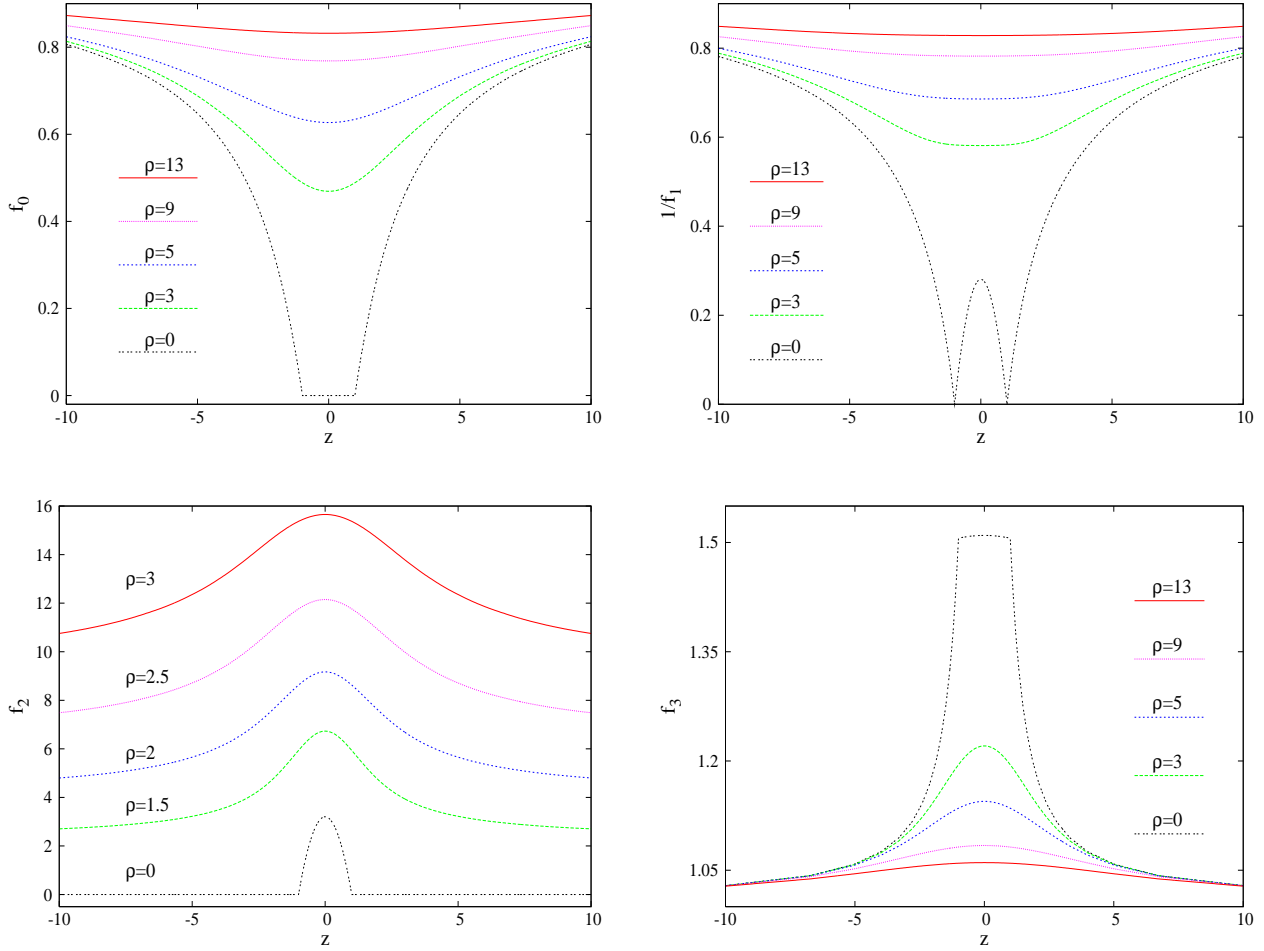


Figure 3. The metric functions f_i of a typical uniform black string solution in EGB theory are shown versus z for several values of ρ . The relevant parameters here are $a = 1$, $\alpha' = 0.175$.

The free parameters in the near horizon expansion are $b_h > 0$ and $\sigma_h > 0$.

The above relations imply the existence of a minimum horizon size for a given value of the GB coupling constant

$$r_h \geq \sqrt{8\alpha'}. \quad (3.18)$$

Since, as discussed in Ref. [20], the horizon radius is decreasing monotonically with the mass of the solutions, the relation (3.18) shows again the existence of a minimal value of the mass for a given GB coupling constant α' .

At infinity, the background approached by a black string is the four-dimensional space-time times the φ -direction, $ds^2 = dr^2 + r^2(d\theta^2 + \sin^2\theta d\psi^2) - dt^2 + d\varphi^2$. The solution as

¹¹It is interesting to notice that this is valid also for solutions with a cosmological constant.

$r \rightarrow \infty$ is written in terms of two parameters c_t, c_z :

$$\begin{aligned} N(r) &= 1 + \frac{c_z - c_t}{r} + \frac{c_t c_z}{4r^2} + O(1/r^3), \quad \sigma(r) = 1 - \frac{c_z}{2r} + \frac{3c_z(c_z - c_t)}{8r^2} + O(1/r^3), \\ b(r) &= 1 + \frac{c_z}{r} + \frac{c_t c_z}{r^2} + O(1/r^3). \end{aligned} \quad (3.19)$$

Similar to the case of Einstein gravity, the EGB black string solutions possess two global charges – the mass M and the tension \mathcal{T} , associated with the Killing vectors $\partial/\partial t$ and $\partial/\partial\varphi$, respectively. These global charges are fixed by the constants c_t, c_z in the asymptotic expansion (3.19):

$$M = \frac{\Delta\varphi}{4\pi G}(2c_t - c_z), \quad \mathcal{T} = \frac{1}{4\pi G}(c_t - 2c_z). \quad (3.20)$$

Without entering into details, we mention that the black string solutions can also be recovered within the metric ansatz (2.12). The coordinate transformation between this ansatz and (3.14) can be worked out in a similar way to (3.8)-(3.12) (note however that $\rho = \frac{1}{2}r_0 \sinh \bar{G}(r) \sin \theta$, and $z = \frac{1}{2}r_0 \cosh \bar{G}(r) \cos \theta$ in this case). These solutions have a semi-infinite space-like rod $[-\infty, -a]$ along the ψ -direction, a finite time-like rod $[-a, a]$ corresponding to the event horizon and a second semi-infinite space-like rod $[a, \infty]$ again in the ψ -direction (thus there is no rod along the φ -direction, see Figure 1c). This can also be seen in Figure 3, where the metric functions f_i of a typical EGB uniform black string solution are shown as a function of z for several values of ρ (one can notice the nontrivial shape of the metric function f_3).

However, the EGB black string solutions are much more difficult to study in the coordinate system (2.12), since in this case one deals with partial differential equations. In particular, it is much more difficult to prove analytically the existence of a maximal value of α' for a given length of the finite timelike rod¹².

4. The static EGB black rings

The physical intuition (supported by the results in the previous Section) suggests that all known solutions in Einstein gravity admit generalizations in EGB theory. While it is rather inconvenient to use the metric ansatz (2.12) for the study of EGB Schwarzschild black holes and EGB black strings, this is not the case for more complicated solutions with a nonspherical topology of the horizon. In fact, in our opinion, the simplest way to construct EGB generalizations of such objects is within the metric ansatz (2.12), by imposing the same rod structure as in the absence of the GB term.

In this Section we present numerical evidence for the existence of static black rings, as the simplest example of an asymptotically flat black object with a nonspherical topology of the horizon in EGB theory.

¹²However, the coordinate system (2.12) makes possible to attempt a numerical construction of more complicated Kaluza-Klein solutions in EGB theory, *e.g.* multi-black strings or configurations with bubbles.

4.1 The static black rings in Einstein gravity

The rod structure of a static black ring solution in Einstein gravity is exhibited in Figure 1b. It consists of a semi-infinite space-like rod $[-\infty, z_1]$ in the ψ -direction (thus $f_2(0, z) = 0$ there), a finite time-like rod $[z_1, z_2]$ ($f_0(0, z) = 0$), a second (and finite) space-like rod $[z_2, z_3]$ in the ψ -direction, where $f_2(0, z) = 0$ again, and a semi-infinite space-like rod $[z_3, \infty]$ ($f_3(0, z) = 0$) in the φ -direction (and $z_1 < z_2 < z_3$).

The metric functions f_i of the static black ring¹³ are given by [2],[22]

$$\begin{aligned} f_0 &= \frac{R_2 + \xi_2}{R_1 + \xi_1}, & f_1 &= \frac{(R_1 + \xi_1 + R_2 - \xi_2)((1-c)R_1 + (1+c)R_2 + 2cR_3)}{8(1+c)R_1R_2R_3}, \\ f_2 &= \frac{(R_2 - \xi_2)(R_3 + \xi_3)}{R_1 - \xi_1}, & f_3 &= R_3 - \xi_3, \end{aligned} \quad (4.1)$$

where

$$\xi_i = z - z_i, \quad R_i = \sqrt{\rho^2 + \xi_i^2} \quad \text{and} \quad z_1 = -a, \quad z_2 = a, \quad z_3 = b, \quad (4.2)$$

a and b being two positive constants, with $c = a/b < 1$. Roughly speaking, a fixes the size of the horizon, while b provides a measure of the radius of the ring's S^1 .

Since the orbits of ψ shrink to zero at $-a$ and a while those of φ do not vanish anywhere there, the topology of the horizon is $S^2 \times S^1$, see Figure 1b (although the S^2 is distorted away from perfect sphericity).

The mass, event horizon area and Hawking temperature of this solution are:

$$M^{(E)} = \frac{3aV_3}{4\pi G}, \quad A_H^{(E)} = 8a^2V_3\sqrt{\frac{2}{a+b}}, \quad T_H^{(E)} = \frac{1}{4\pi a}\sqrt{\frac{a+b}{2}}. \quad (4.3)$$

Although the static black ring solution is asymptotically flat¹⁴, it contains a conical singularity for the finite ψ -rod, since δ as defined by (2.27) is nonzero:

$$\delta = 2\pi \left(1 - \sqrt{\frac{b+a}{b-a}} \right). \quad (4.4)$$

One can easily see that this is a negative quantity, $\delta < 0$, which implies the existence of a two-dimensional disk-like deficit membrane (with negative deficit) that prevent the configuration from collapsing.

Another quantity of interest is the area of the spacetime spanned by the conical singularity and the proper length of the finite ψ -rod, which are computed according to (2.29), (2.25):

$$Area = \beta \frac{2\pi(b-a)^{3/2}}{\sqrt{a+b}}, \quad L = \sqrt{2}\sqrt{b-a} E(n), \quad (4.5)$$

¹³Note that the function $f_1(0, z)$ behaves as $1/|z - z_i|$ as $z \rightarrow z_i$.

¹⁴The Einstein gravity static black ring solution in [2] admits an alternative interpretation as a ring sitting on the rim of a membrane that extends to infinity. (This is found by requiring that the periodicity of ψ is 2π on the finite ψ -rod.) However, the asymptotic metric is a deficit membrane in this case.

where $n = (b - a)/(b + a)$, $E(n)$ being the complete elliptic integral of the second kind.

In terms of the dimensionless parameter a/b , one may think of a static black ring as interpolating between two limits. As $a/b \rightarrow 1$, the finite ψ -rod vanishes and the Schwarzschild metric is approached, with $\delta \rightarrow -\infty$. As $a/b \rightarrow 0$, the second ψ -rod extends to infinity and the solution becomes, after a suitable rescaling¹⁵, a black string, *i.e.* the four dimensional Schwarzschild black hole uplifted to five dimensions.

4.2 The static black rings in EGB theory

4.2.1 The ansatz and the physically relevant quantities

The EGB generalizations of the Emparan-Reall black rings are found by solving the EGB equations for the metric ansatz (2.12).

The boundary conditions satisfied by the EGB black ring metric functions are similar to those in Einstein gravity. At $\rho = 0$, the function f_0 vanishes for $-a \leq z \leq a$ (*i.e.* on the horizon), f_2 is zero for $-\infty \leq z \leq -a$ and $a \leq z \leq b$, while f_3 vanishes for $z \geq b$. As a result, along the horizon the orbits of ψ shrink to zero at $z = -a$ and $z = a$, while the orbits of φ do not shrink to zero anywhere. Thus the topology of the horizon is $S^2 \times S^1$. From (2.18), (2.19), one can see that, for a given rod with one of the functions vanishing, $f_a = 0$, the other f_i satisfy Neumann-type boundary conditions, $\partial_\rho f_i|_{\rho=0} = 0$ (with $i \neq a$). At infinity, we require that the functions f_i approach the Minkowski form (2.13).

In practice, we have found it convenient to take

$$f_i = f_i^0 F_i, \quad (4.6)$$

where f_i^0 are background functions, given by the metric functions of the Einstein gravity black ring solution (4.1). The advantage of this approach is that the f_i will automatically satisfy the desired rod structure. Moreover, this choice ‘absorbes’ the divergencies of the functions f_2 and f_3 as $r \rightarrow \infty$ coming from the imposed asymptotic behaviour.

The equations satisfied by the F_i can easily be derived from the general set of EGB equations¹⁶. As for the boundary conditions, the relations (2.18), (2.19) together with the expressions (4.1) of the background functions f_i^0 imply

$$\partial_\rho F_i|_{\rho=0} = 0, \quad \text{for } -\infty < z < \infty,$$

and $F_i = 1$ as $\rho \rightarrow \infty$ or $z \rightarrow \pm\infty$.

The constraint equation $E_\rho^z = 0$ results in $F_2/F_1 = \text{const.}$ on the ψ -rods. Now, to be consistent with the assumption of asymptotic flatness, one finds $\text{const.} = 1$ for $-\infty < z \leq -a$. The value of this ratio for the second rod with $a < z \leq b$ is obtained only as a result of the numerical solution. A similar reasoning implies $F_3/F_1 = 1$ on the φ -rod ($b \leq z \leq \infty$).

¹⁵For the line element used in this work, this rescaling is $r \rightarrow \sqrt{2b}\bar{r}$, $z \rightarrow \sqrt{2b}\bar{z}$, $\varphi \rightarrow \bar{\varphi}/\sqrt{2b}$ together with $a \rightarrow \sqrt{2b}\bar{a}$.

¹⁶Note, however, that the field equations become much more complicated in terms of the F_i , with the number of terms increasing drastically.

All of the physically relevant quantities except for the mass are encoded in the values of the functions F_i, f_i^0 at $\rho = 0$. The event horizon area of static black rings in EGB theory is given by

$$A_H = \Delta\psi 2\pi \int_{-a}^a dz \sqrt{f_1 f_2 f_3} = \Delta\psi 4\pi a \sqrt{\frac{2}{a+b}} \int_{-a}^a dz \sqrt{(b-z)F_1 F_2 F_3}, \quad (4.7)$$

where $\Delta\psi$ is the periodicity of the angular coordinate ψ on the horizon.

The Hawking temperature can be computed from the surface gravity or by requiring regularity on the Euclidean section

$$T_H = \frac{1}{4\pi a} \sqrt{\frac{a+b}{2}} \sqrt{\frac{F_0}{F_1}}, \quad (4.8)$$

where the constraint equation E_ρ^z guarantees that the ratio F_0/F_1 is constant on the event horizon.

At infinity, the five dimensional Minkowski background is approached, with $\Delta\psi = 2\pi$ there. From (2.20), the mass M of the solutions can be read from the subleading term in the asymptotic expansion for $f_0 = f_0^0 F_0$. To obtain a Smarr-like relation (which is useful in numerics, see Appendix B.2), we consider the EGB equation $E_t^t = G_t^t + \alpha' H_t^t = 0$ in the form $R_t^t = 1/2R - \alpha' H_t^t$ and integrate over a spacelike hypersurface. The volume integral on the left hand side of the equation reduces to surface integrals at the horizon and at infinity, which can be evaluated in terms of the mass, area and Hawking temperature,

$$\int R_t^t \sqrt{-g} d^4x = \frac{1}{2} \left(2\pi T_H A_H - \frac{16\pi}{3} GM \right). \quad (4.9)$$

Substituting this expression on the left hand side and solving for the mass yields

$$16\pi GM = 6\pi T_H A_H + I_{\alpha'} = 6\pi T_H A_H - 3 \int \{R - 2\alpha' H_t^t\} \sqrt{-g} d^4x. \quad (4.10)$$

In the limit $\alpha' \rightarrow 0$ the integral $I_{\alpha'}$ vanishes and the relation reduces to the usual Smarr relation.

To further characterize the properties of the horizon, we introduce the minimal and maximal S^1 horizon radii, R_{\min} and R_{\max} , defined via

$$R_{\min} = \frac{1}{2\pi} \int_0^{2\pi} \sqrt{g_{\varphi\varphi}}|_{\rho=0, z=a} d\varphi = \sqrt{2(b-a)F_3(0, a)}, \quad (4.11)$$

$$R_{\max} = \frac{1}{2\pi} \int_0^{2\pi} \sqrt{g_{\varphi\varphi}}|_{\rho=0, z=-a} d\varphi = \sqrt{2(b+a)F_3(0, -a)}. \quad (4.12)$$

Turning now to the finite ψ -rod, we note that all solutions we have found have $F_2/F_1 \neq 1 - 2a/(b+a)$ here. Thus, from (2.27), the coordinate ψ possesses a conical excess for

$a \leq z \leq b$, which is¹⁷

$$\delta = 2\pi \left(1 - \sqrt{\frac{b+a}{b-a}} \sqrt{\frac{F_2}{F_1}} \right). \quad (4.13)$$

The proper length of the finite ψ -rod is given by

$$L = \int_a^b dz \sqrt{f_1(0, z)} = \sqrt{\frac{b-a}{2(b+a)}} \int_a^b dz \sqrt{\frac{a+z}{(z-a)(b-z)}} \sqrt{F_1(0, z)}. \quad (4.14)$$

Of interest is also the expression for the space-time area spanned by the conical singularity,

$$Area = 2\pi\beta \int_a^b dz \sqrt{f_1(0, z) f_3(0, z) f_0(0, z)} = 2\pi\beta \sqrt{\frac{b-a}{b+a}} \int_a^b dz \sqrt{F_1(0, z) F_3(0, z) F_0(0, z)}. \quad (4.15)$$

The GB correction $Area_1/\beta$ to the parameter \mathcal{A} which enters the thermodynamics can also be computed from (2.37), (4.1). is $A = Area/\beta$.

4.2.2 The numerical results

In the absence of analytical methods to construct EGB black rings, a numerical approach of this problem seems to be a reasonable task. We have solved the resulting set of four coupled nonlinear elliptic partial differential equations numerically, subject to the above boundary conditions. Details on the numerical methods used and on a new coordinate system better suited for the numerical study of these solutions are presented in Appendix B.

The problem has two dimensionless parameters, which we have chosen to be b/a and α'/a . We note that solutions are equivalent under scaling

$$(a, b, \alpha') \rightarrow (\lambda^2 a, \lambda^2 b, \lambda^2 \alpha').$$

Mass, area, temperature etc. scale according to their dimensions

$$(M, A_H, T_H, \dots) \rightarrow (\lambda^2 M, \lambda^3 A_H, \lambda^{-1} T_H, \dots)$$

With $\lambda^2 = 1/a$ we obtain the dimensionless quantities

$$\hat{M} = M/a, \hat{A}_H = A_H/a^{3/2}, \hat{T}_H = a^{1/2} T_H, \dots$$

Starting from black rings of Einstein gravity, we have generated branches of EGB black rings by increasing the GB coupling constant α from zero, while keeping the parameters a and b fixed. Typical profiles of the solutions are presented in Figures 4 and 5. We note that the functions F_i are smooth outside of the z -axis, showing no sign of a singular behaviour.

¹⁷The coordinate ψ can of course be rescaled such that its periodicity is 2π on the finite ψ -rod. Then the interpretation of the solutions is somehow different, since they would describe a static ring sitting on the rim of a deficit membrane that extends to infinity (in which case $\delta > 0$). Since for this choice the spacetime is not asymptotically flat, we have preferred to consider the case of a conical singularity localized in the bulk.

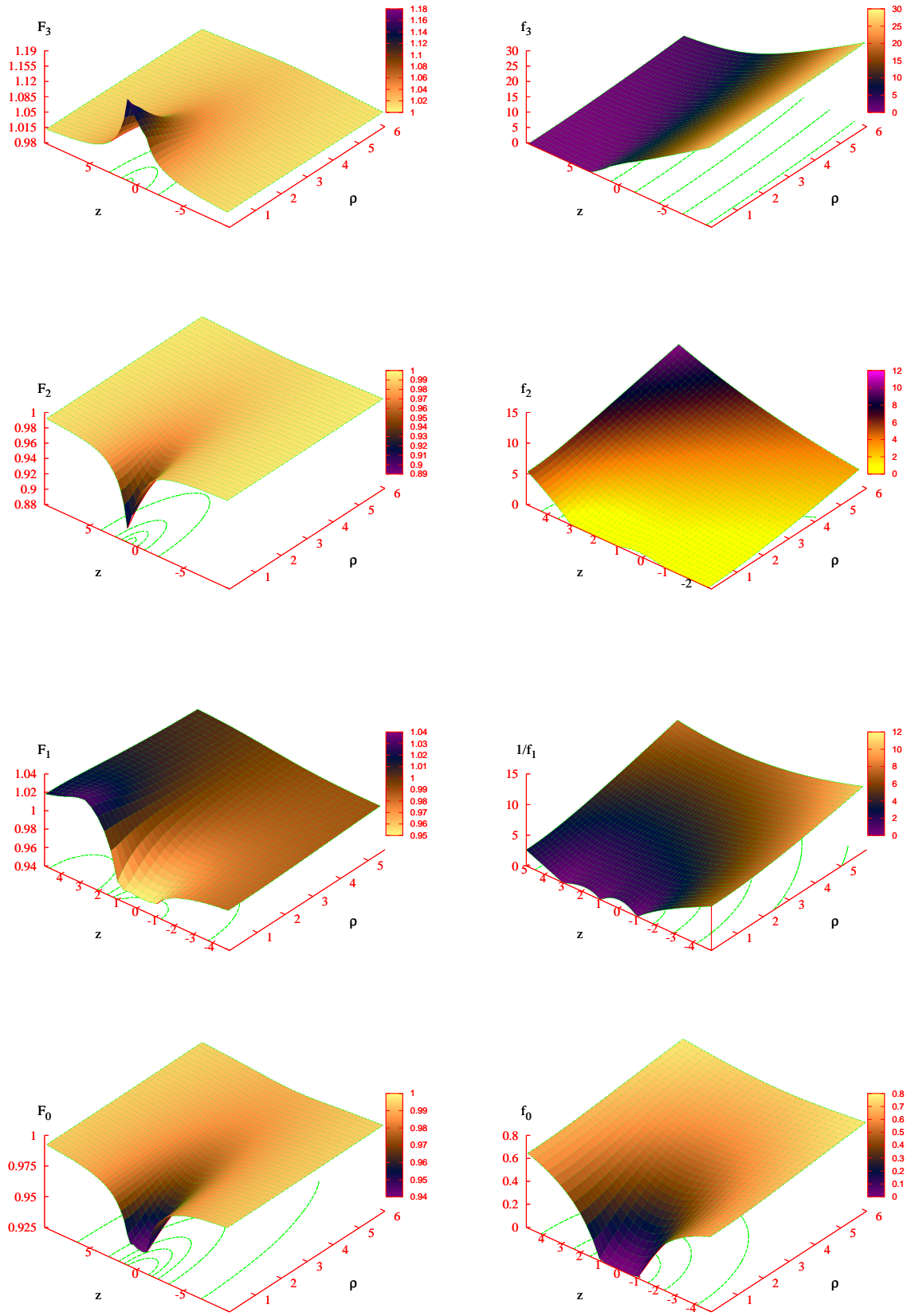


Figure 4. The profiles of the functions F_i employed in the numerical calculations and of the metric functions f_i are shown for a typical EGB black ring solution with $a = 1$, $b = 3$, $\alpha' = 0.0125$.

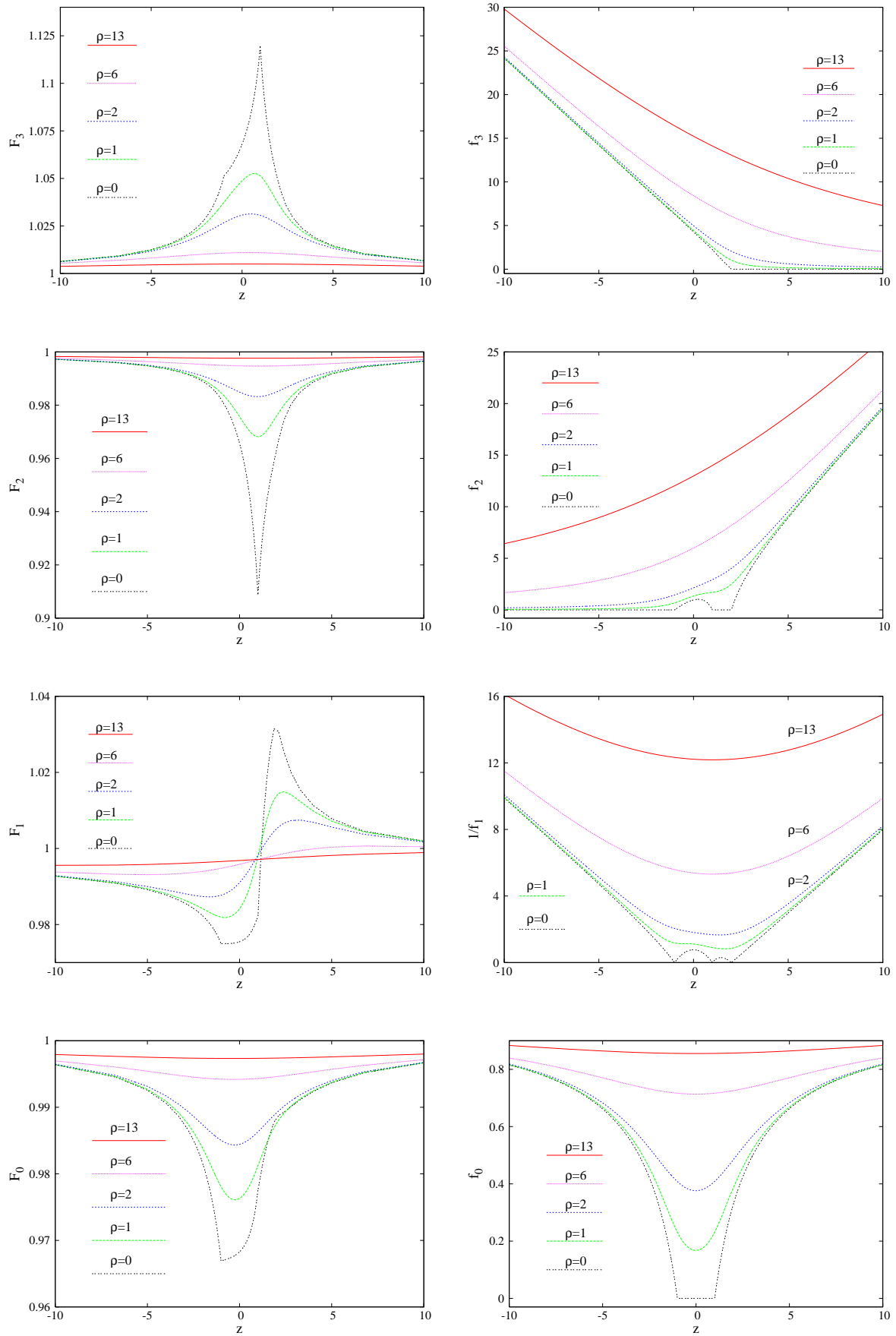


Figure 5. The profiles of the functions F_i used in numerics and of the metric functions f_i are shown as functions of z for several values of ρ for a black ring solution with $a = 1$, $b = 2$, $\alpha' = 0.01$.

The crucial point here is that the divergent behaviour of the functions f_i has already been subtracted by the background functions f_i^0 . We have verified that the Kretschmann scalar stays finite everywhere, in particular at $\rho = 0$.

A number of basic features of these EGB black ring solutions are analogous to those of the static black rings of Einstein gravity. In particular, all solutions have a conical excess δ on the finite ψ -rod (for the choice of $\Delta\psi = 2\pi$ at infinity). Moreover, on the horizon the circumference of the S^1 is maximum for $z = -a$ and minimum for $z = a$.

The isometric embedding of the horizon is shown in Figure 6 for a family of EGB black ring solutions with fixed parameters $a = 1$ and $\alpha' = 0.015$ and several values of b , chosen in the interval $1.1 \leq b \leq 8$.

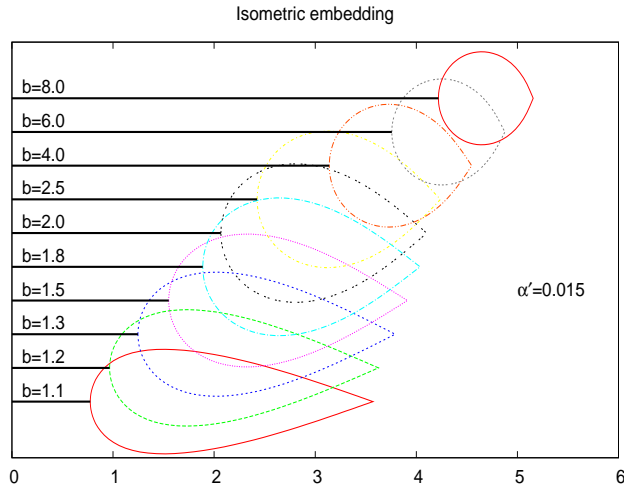


Figure 6. The embedding of the EGB black ring horizon for a family of solutions with $a = 1$, $\alpha' = 0.015$ and several values of the parameter b . Note, that the conical singularity has been moved to the outside of the ring, stretching from its surface to infinity.

We note, that for this embedding the conical singularity was moved from the finite ψ -rod to the exterior of the ring, extending from the outer ring circumference (at the maximal radius R_{\max}) to infinity¹⁸. Therefore the horizon is smooth and round at the inner circumference of the ring, while it exhibits a cone-like edge at the outer circumference at the maximal radius R_{\max} . As the parameter b is increased, the proper distance from the center of the ring to the horizon increases. At the same time the conical excess decreases. Consequently, the shape of the horizon becomes more and more spherical with increasing b .

Thus, for a given α' , one might hope that the conical excess could be completely removed, by going to large enough values of b . This hope, however, is dashed, when the parameter space is fully explored.

Whereas for Einstein black rings the ratio $c = a/b$ exploits the full range $0 \leq c \leq 1$,

¹⁸Note that for the choice $\Delta\phi = 2\pi$ at infinity the embedding would be pseudo-Euclidean.

EGB black rings are restricted to the $\hat{\alpha}'$ -dependent range

$$0 < c_{\min}(\hat{\alpha}') \leq c \leq c_{\max}(\hat{\alpha}') < 1. \quad (4.16)$$

For a given $\hat{\alpha}' = \alpha'/a$, these minimal and maximal values of c can be read from Figure 7. This figure, which is one of the central results of this paper, exhibits the maximal value of the scaled coupling $\hat{\alpha}'$, up to which EGB black rings can be obtained for a fixed value of the parameter ratio $c = a/b$. Therefore it delimits the domain of existence of EGB black rings. The coupling $\hat{\alpha}'$ approaches its maximum value approximately in the middle of the interval, *i.e.* for $a/b \simeq 1/2$.

As $\hat{\alpha}' \rightarrow \hat{\alpha}'_{\max}$, the numerical process fails to converge, although no singular behaviour is found there. This result is not a surprise given the black ring – black string connection. Heuristically, these EGB black ring solutions may be thought of as being obtained by taking a piece of the EGB black string and forming a circle. Thus they would inherit the $r_h - \alpha'$ constraint (3.18) from there. The technical reason which causes the solutions to cease to exist at $\hat{\alpha}'_{\max}$ is discussed in Appendix B.3. It involves an analytic explanation of this fact based on a computation performed in a special coordinate system introduced there. Similar to the black string case, the argument in the Appendix uses an analysis of the field equations at the event horizon.

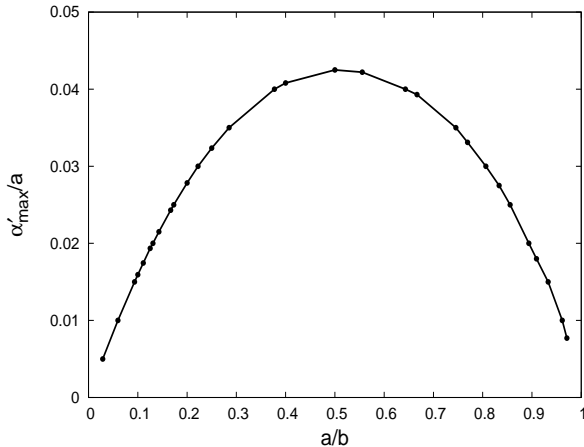


Figure 7. The domain of existence of EGB black rings is delimited by the maximal value of $\hat{\alpha} = \alpha'/a$ versus the parameter ratio $c = a/b$.

In Figure 8 a number of physically relevant properties of the EGB black rings are exhibited as functions of the scaled coupling $\hat{\alpha}'$ for a family of values of the ratio b/a . Also included are the curves, showing the values of the respective properties on the boundary of the domain of existence of the EGB black rings.

The first quantity shown is the relative conical excess $\bar{\delta}$. Only for $\alpha' = 0$, it covers the full range $-1 \leq \bar{\delta} \leq 0$. Thus it always differs from zero in the domain of existence of EGB black rings, as pointed out above.

The scaled mass $\hat{M} = M/a$ is constant for the Einstein black rings, since it depends only on a . Therefore the EGB mass curves start for all values of b/a from this Einstein

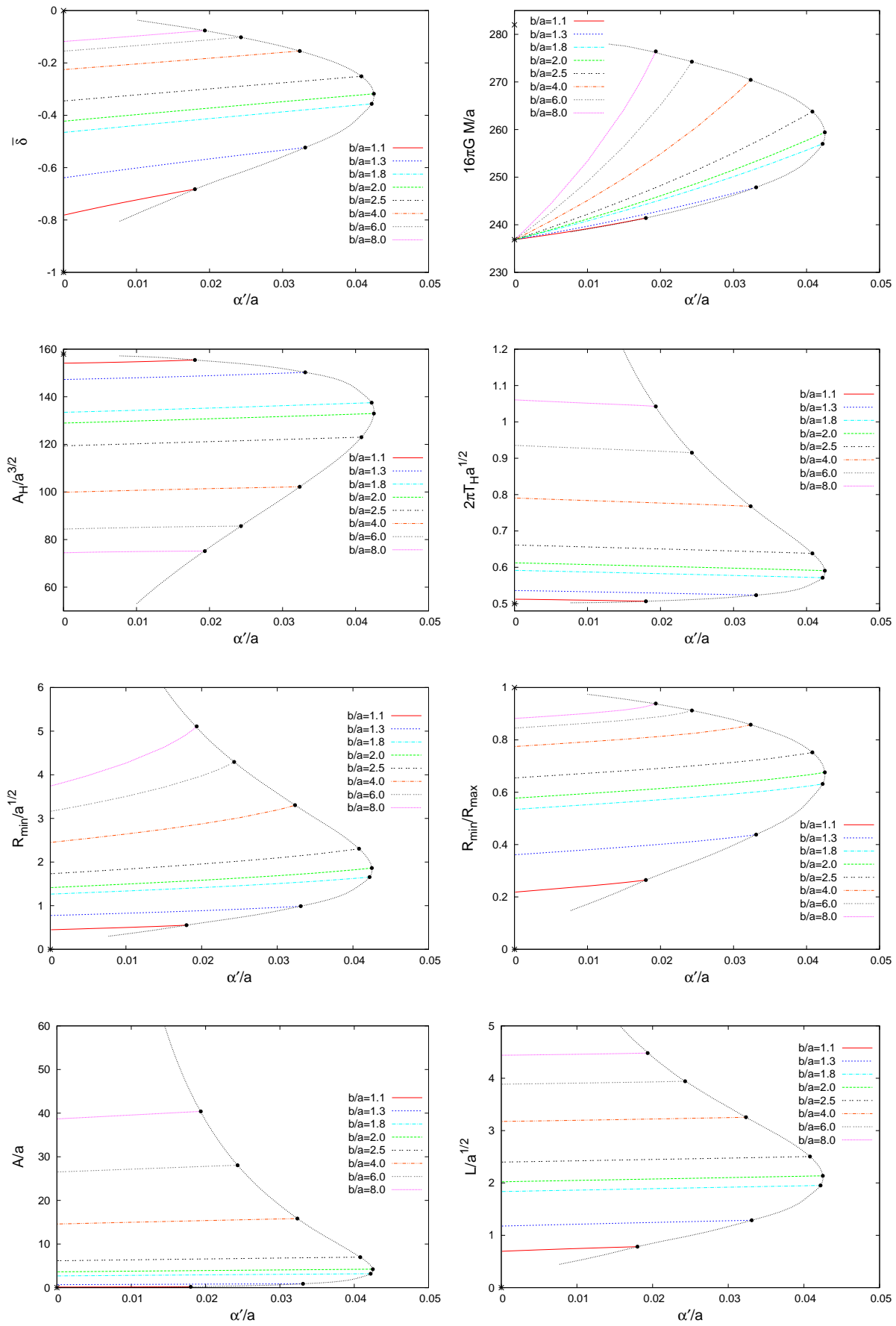


Figure 8. Several physically relevant (scaled) quantities are shown versus $\hat{\alpha}'$ for several fixed values of b/a . The asterisks and crosses indicate the limits $b/a \rightarrow 1$, respectively $b/a \rightarrow \infty$

value and increase monotonically until they reach the boundary of the domain of existence at the respective maximal value of α'/a .

The maximal value of the mass, reached on the boundary for $b/a \rightarrow \infty$, is finite and less than 20% above the Einstein value. Recalling the Smarr-like formula (4.10) for the mass, we conclude that this increase of the mass is basically due to the integral $I_{\alpha'}$.

The scaled event horizon area $\hat{A}_H = A_H/a^{3/2}$ increases slightly with the coupling α'/a . Its boundary line starts from the finite maximal value of the Schwarzschild black hole at $b/a = 1$. Extrapolating the solutions on the boundary to the limit $b/a \rightarrow \infty$, we observe that the values of \hat{A}_H of the solutions on the boundary tend to zero as $\sqrt{\alpha'/a}$.

The scaled temperature $\hat{T}_H = a^{1/2}T_H$ on the other hand exhibits a slight decrease with α'/a . (However, the solutions are far away from extremality.) The boundary line for the temperature starts from the finite minimal value of the Schwarzschild black hole at $b/a = 1$. Extrapolation this boundary line to the limit $b/a = \infty$ shows, that the values of \hat{T}_H on the boundary tend to infinity as $1/\sqrt{\alpha'/a}$. Consequently, the product of \hat{A}_H and \hat{T}_H , entering the Smarr-like formula (4.10), stays finite in the limit.

The inner and outer radii of the ring, R_{\min} and R_{\max} , exhibit a more pronounced dependence on $\hat{\alpha}'$, in particular for larger values of the ratio b/a . The figure exhibits besides the scaled minimal radius \hat{R}_{\min} also their ratio R_{\min}/R_{\max} . The boundary line of the ratio starts from the Schwarzschild black hole value $R_{\min}/R_{\max} = 0$ and ends at the maximally reachable value of $R_{\min}/R_{\max} = 1$.

Figure 8 also shows the scaled proper length \hat{L} of the ψ -rod and the scaled thermodynamical parameter \hat{A} . For these quantities we observe only a small dependence on $\hat{\alpha}'$, increasing with $\hat{\alpha}'$ only by a few percent for fixed b/a . A similar picture has been found for the quantities A_1 and $Area_1$, as given by (2.35), (2.37), respectively.

Finally, we would like to return to the intriguing observation, that the conical excess δ decreases with increasing the GB coefficient $\hat{\alpha}'$. While this result has been unexpected (for us), it can be heuristically understood as follows. In the presence of curvature-squared terms, the modified Einstein equations leads to an effective stress tensor that involves the gravitational field

$$G_{\mu\nu} = -\alpha' H_{\mu\nu} = T_{\mu\nu}. \quad (4.17)$$

Therefore, from some point of view, the quantity $\alpha'H_t^t (= -G_t^t)$ corresponds to a local ‘effective energy density’. However, this effective stress tensor, thought of as a kind of matter distribution, in principle may violate the weak energy condition¹⁹. This is indeed the case, since as one can see in Figure 9, near the horizon this quantity takes negative values in some region of the $\rho - z$ plane. The picture is however quite complicated and depends in a nontrivial way on the value of the input parameters a/b and $\hat{\alpha}'$. For fixed $\hat{\alpha}'$ and a value of the ratio a/b close to one, the region with a negative ‘effective energy density’ is localized around the topology changing point at $\rho = 0$, $z = b$. This region expands when the ratio a/b is decreased. For sufficiently large values of b a more complicated picture

¹⁹This mechanism has been exploited to construct wormhole solutions in $d = 5$ EGB theory, see the discussion in [17] and the references there.

emerges, with the occurrence of another region where $\alpha' H_t^t < 0$, which is localized around the horizon²⁰.

We conclude that, for a black ring, the contribution of the Gauss-Bonnet provides a repelling force in addition to that supplied by the conical excess. While this, in principle, might have given hope to construct balanced static black rings in EGB theory, these could unfortunately not be realized, since the solutions cease to exist before the limit $\delta = 0$ is reached.

4.2.3 The large b limit and the maximal coupling $\alpha'_{s,\max}$

Let us now address the large b limit and try to understand the character of the solutions obtained along the boundary of the domain of existence, when the ratio a/b tends to zero along with the coupling $\hat{\alpha}'$.

In Figure 10 we show the ratio $\mu = 16\pi GM/6\pi A_H T_H$ versus the ratios R_{\min}/R_{\max} and a/b for several values of α' . The dots indicate solutions on the boundary of the domain of existence. They represent solutions with the maximal and minimal values for the ratio b/a for a fixed value of the coupling $\hat{\alpha}'$.

We note that with decreasing $\hat{\alpha}'$ the maximal value of a/b increases. Here we expect to reach the five dimensional Schwarzschild solution as $\hat{\alpha}'$ tends to zero and b tends to a . In this limit the ratio μ assumes the value $\mu = 1$.

On the other hand, the minimal value of a/b decreases with decreasing $\hat{\alpha}'$, and tends to zero as $\hat{\alpha}'$ tends to zero, whereas the ratio μ tends to a finite value in this limit. In the following we show that in this limit the (suitably scaled) EGB uniform black string at its maximal value of α' is approached.

For comparison with the black rings, we have performed a systematic study of the EGB uniform black strings. Here we have used a coordinate system which is different from (3.14), being related to a limit of the metric ansatz introduced in Appendix B. The line element of the black strings is parametrized as

$$ds^2 = -f(r)dt^2 + m(r) (dr^2 + r^2 d\Omega_2^2) + l(r)d\phi^2 . \quad (4.18)$$

(Note that the $d = 4$ reduction along the ϕ -direction gives black holes in isotropic coordinates.)

As noted above, the mass and tension of the black strings can be expressed in terms of the coefficients entering the asymptotic expansion of the g_{tt} and $g_{\phi\phi}$ components of the metric. Thus, from $-g_{tt} \approx 1 - \frac{c_t}{r}$, $g_{\phi\phi} \approx 1 + \frac{c_\phi}{r}$, we obtain

$$M_s/\Delta\phi = M_* + \frac{1}{2}\mathcal{T}, \quad \mathcal{T} = \frac{1}{4\pi G}(c_t - 2c_\phi), \quad (4.19)$$

with

$$M_* = \frac{1}{4\pi G} \frac{3}{2} c_t . \quad (4.20)$$

²⁰We have noticed a similar picture for EGB black strings. For all solutions there we have found $H_t^t < 0$ for a region near the horizon. However, the picture is different for the EGB black holes, in which case one can prove that H_t^t is always a positive quantity. A deeper understanding of this difference is still missing.

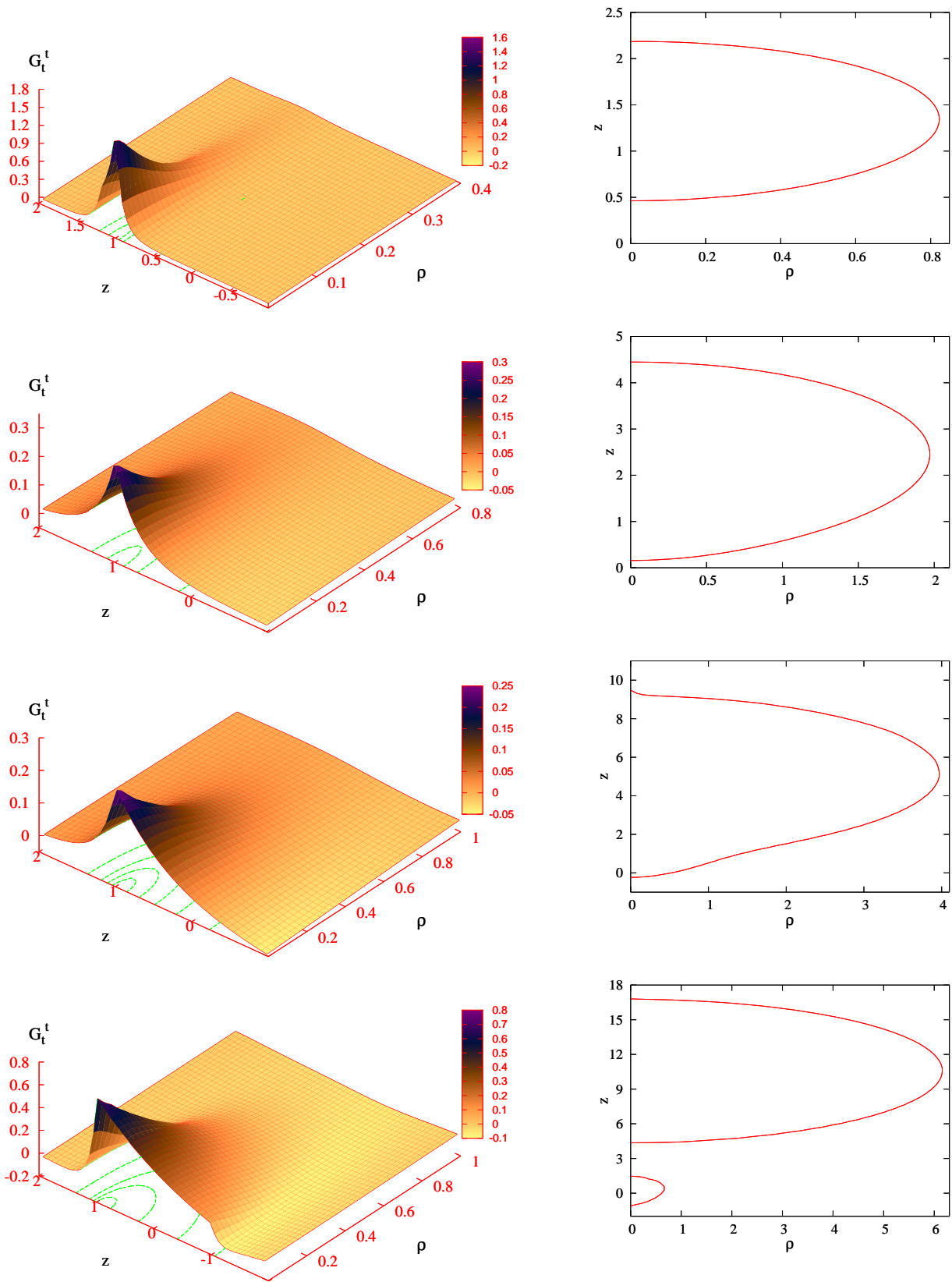


Figure 9. Left column: The G_t^t component of the Einstein tensor near the horizon versus ρ and z for $\alpha' = 0.015$, $a = 1$ and $b = 1.2, 2.0, 4.0$ and 8.0 from top to bottom. Right column: The curve $G_t^t = 0$ versus ρ and z for the same set of parameters.

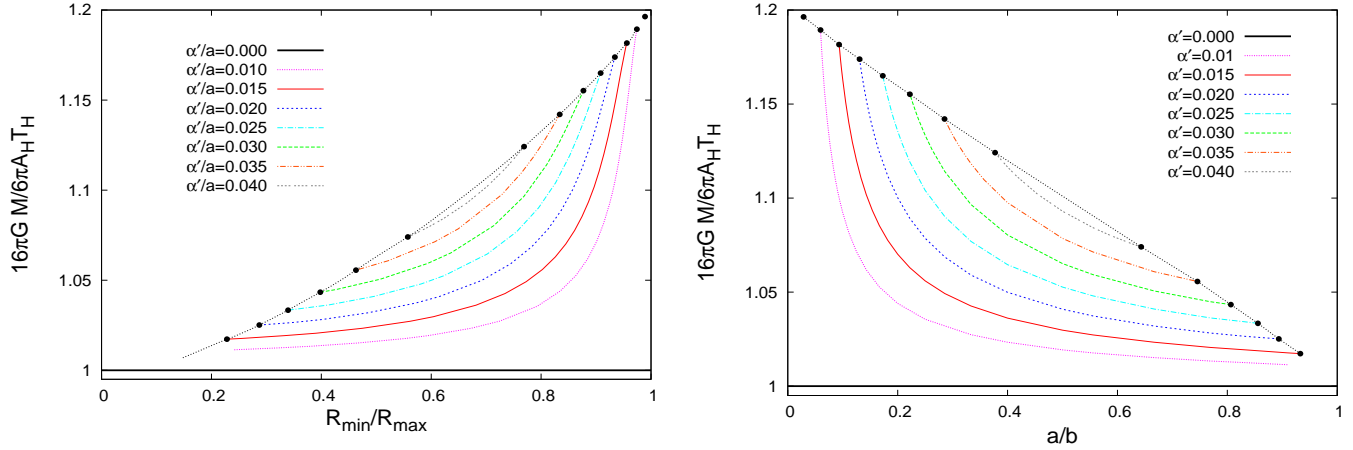


Figure 10. The dimensionless ratio $16\pi GM/6\pi A_H T_H$ is shown versus the ratios R_{min}/R_{max} and a/b , respectively, for several values of α' .

The Hawking temperature and horizon area of a black string are obtained as

$$T_H^s = \frac{1}{2\pi r_0} \sqrt{\frac{\hat{f}}{m}} \Big|_{r_0}, \quad A_H^s = 4\pi r_0^2 \Delta\phi m \sqrt{l} \Big|_{r_0}, \quad (4.21)$$

where r_0 and $\Delta\phi$ denote the isotropic horizon radius and the length of the compact coordinate, respectively, and the function $\hat{f}(r) = f(r)/(1 - r_0/r)^2$ is finite at the horizon. For fixed values of r_0 , uniform black string solutions exist for all $\alpha'_s/r_0^2 < \alpha'_{s,max}/r_0^2 \approx 1.44$.

Let us now connect the uniform black strings with the black rings in the limit $a/b \rightarrow 0$. From the results for the black rings (e.g. Figure 7) we observe that the product $\alpha' b_{max}(\alpha')/a^2$ assumes a finite value when $\alpha'/a \rightarrow 0$ and $b_{max}/a \rightarrow \infty$, which corresponds precisely to a fraction of the scaled maximal string coupling α'_s/r_0^2 , i.e. $\alpha' b_{max}(\alpha')/a^2 \rightarrow \alpha'_{s,max}/8r_0^2$.

We therefore introduce the scaling parameter $\lambda = r_0\sqrt{8b}/a$ such that the scaled coupling $\bar{\alpha}' = \lambda^2\alpha' = 8br_0^2\alpha'/a^2$ tends to $\alpha'_{s,max}$ for $a/b \rightarrow 0$. The scaled parameters

$$\bar{a} = \lambda^2 a = r_0^2 \frac{8b}{a}, \quad \bar{b} = \lambda^2 b = r_0^2 \frac{8b^2}{a^2}$$

then tend to infinity as $b/a \rightarrow \infty$ for fixed a . However, the ratio $\bar{a}/\sqrt{2\bar{b}} = 2r_0$ remains finite in this limit.

In order to obtain the uniform black string limit we also need to scale the angle variable ϕ for the black rings, since the function f_3 also diverges in the limit. Introducing $\bar{\phi} = \sqrt{2\bar{b}}\phi = 4r_0\phi b/a$ and integrating then yields $\Delta\bar{\phi} = 8\pi r_0 b/a$, which is the equivalent of the asymptotic length of the compact dimension. With this expression we thus find for the black rings the scaled Hawking temperature \bar{T}_H , the scaled area per asymptotic length

$\bar{A}_H/\Delta\bar{\phi}$, and the scaled mass per asymptotic length $\bar{M}/\Delta\bar{\phi}$,

$$\begin{aligned}\bar{T}_H &= T_H/\lambda = \frac{a}{\sqrt{8b}} \frac{1}{r_0} T_H \\ \bar{A}_H/\Delta\bar{\phi} &= \lambda^3 A_H/\Delta\bar{\phi} = \frac{r_0^2}{\pi} \sqrt{\frac{8b}{a}} A_H/a^{3/2}, \\ \bar{M}/\Delta\bar{\phi} &= \lambda^2 M/\Delta\bar{\phi} = \frac{r_0}{\pi} M/a,\end{aligned}$$

In Figure 11 we show the inverse of the dimensionless Hawking temperature $\tilde{T}_H = \bar{T}_H r_0$ and the dimensionless area $\tilde{A}_H = \bar{A}_H/\Delta\bar{\phi} r_0^2$ of the black rings on the boundary of their domain of existence versus the scaled coupling constant $\tilde{\alpha}' = \bar{\alpha}'/r_0^2$. Also shown are the corresponding dimensionless $\tilde{T}_H^s = T_H^s r_0$ and $\tilde{A}_H^s = A_H^s/\Delta\phi r_0^2$ of the uniform black string solutions versus the scaled coupling constant $\tilde{\alpha}'_s = \bar{\alpha}'_s/r_0^2$. We observe that \tilde{T}_H and \tilde{T}_H^s assume the same limiting values, when the maximal $\tilde{\alpha}'$ resp. $\tilde{\alpha}'_s$ is approached. The same holds for the dimensionless entropies \tilde{A}_H and \tilde{A}_H^s . We note, that for the black rings the values for $\bar{\alpha}' = \alpha'_{s,\max}$ are extrapolated. The figure also demonstrates, that the product $\tilde{A}_H \tilde{T}_H$ has only a very slight α' -dependence, i.e. for finite α' it differs only slightly from its pure Einstein value (which is 4).

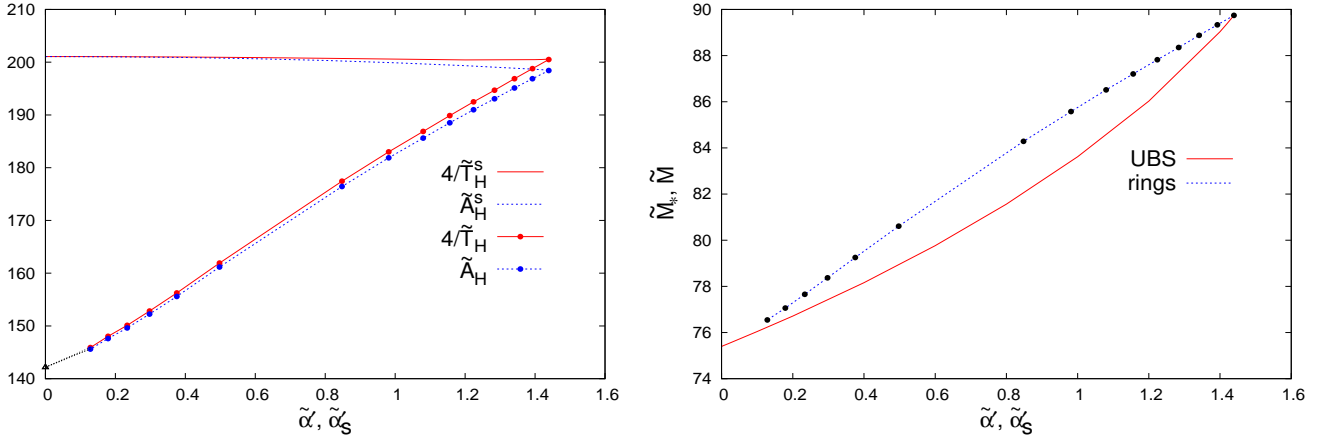


Figure 11. Left: The inverse of the dimensionless Hawking temperature $\tilde{T}_H = T_H r_0$ and the dimensionless area $\tilde{A}_H = \bar{A}_H/\Delta\bar{\phi} r_0^2$ of the black rings on the boundary of their domain of existence and the dimensionless Hawking temperature $\tilde{T}_H^s = T_H^s r_0$ as well as the dimensionless area $\tilde{A}_H^s = A_H^s/\Delta\phi r_0^2$ of the uniform black strings are shown versus $\tilde{\alpha}' = \bar{\alpha}'/r_0^2$ and $\tilde{\alpha}'_s = \bar{\alpha}'_s/r_0^2$, respectively. Right: The same for the dimensionless mass $\tilde{M} = \bar{M}/\Delta\bar{\phi} r_0$ of the black rings and the dimensionless mass $\tilde{M}_* = M_*/r_0$ of the black strings.

To compare the scaled mass of the black rings with the mass of the uniform black strings we have to keep in mind that the former are derived for an asymptotically flat space-time and therefore have no contribution from the tension. Consequently, the relevant quantity of the uniform black strings to compare with is M_* in Eq. (4.20). In Figure 11 we also show the dimensionless masses $\tilde{M} = \bar{M}/\Delta\bar{\phi} r_0$ and $\tilde{M}_* = M_*/r_0$ as functions of $\bar{\alpha}'/r_0^2$ and $\bar{\alpha}'_s/r_0^2$,

respectively. We observe that both masses assume the same values in the limit where the couplings α'_s and $\bar{\alpha}'$ tends to the maximal value $\alpha'_{s,max}$.

4.2.4 The phase diagram

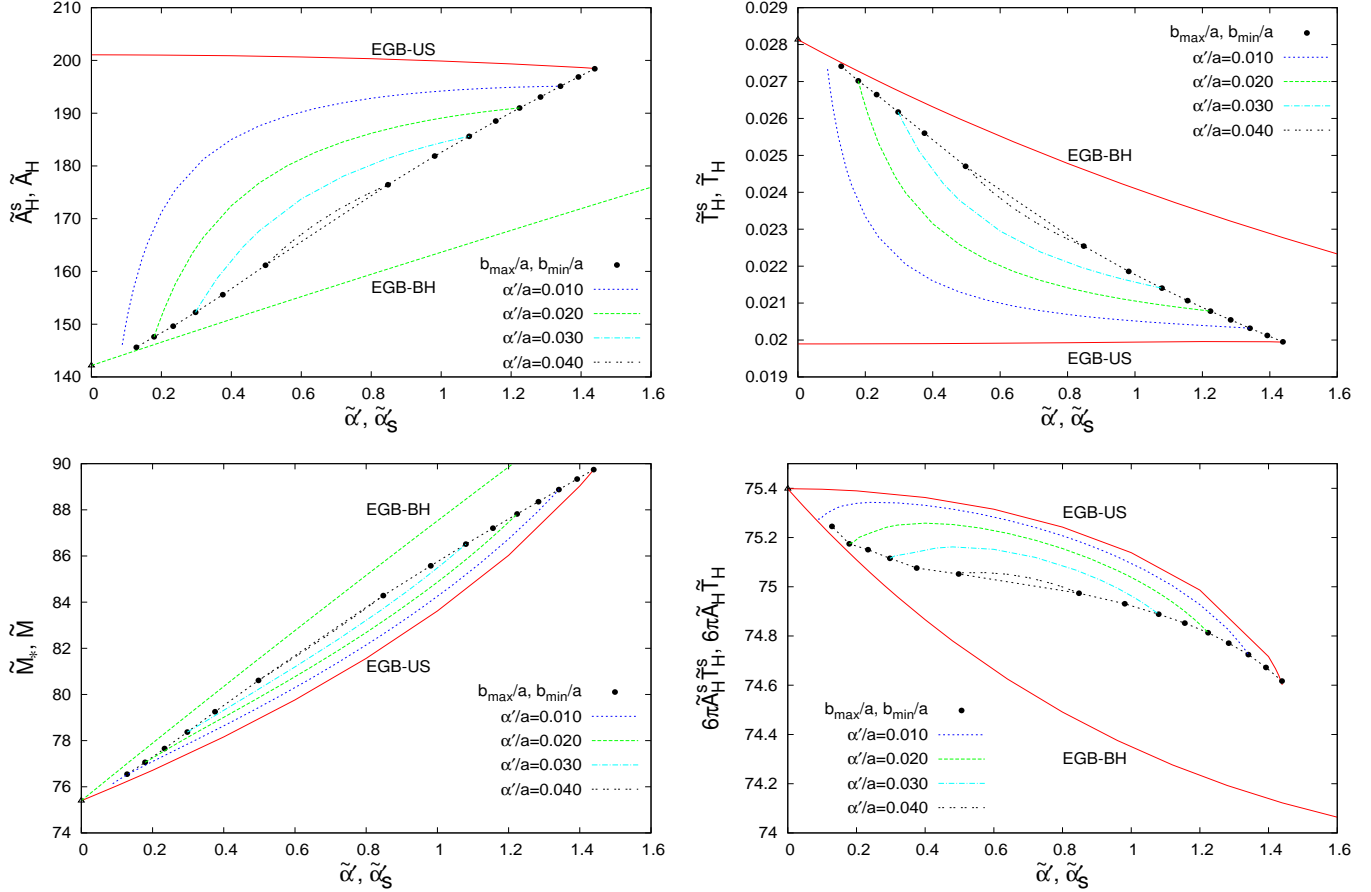


Figure 12. The dimensionless area \tilde{A}_H , temperature \tilde{T}_H , mass \tilde{M}_H , and the product $\tilde{A}_H\tilde{T}_H$ of the EGB black rings and Schwarzschild black holes versus $\tilde{\alpha}' = \bar{\alpha}'/r_0^2$ as well as the respective dimensionless quantities \tilde{A}_H^s , \tilde{T}_H^s , \tilde{M}_H^s and $\tilde{A}_H^s\tilde{T}_H^s$ of the uniform black strings versus $\tilde{\alpha}'_s = \alpha'_s/r_0^2$.

Let us now compare the properties of the three types of static solutions, the EGB Schwarzschild black holes, the EGB black rings and the EGB black strings. To obtain a phase diagram for these solutions we exhibit the dimensionless quantities \tilde{A}_H , \tilde{T}_H , and \tilde{M}_H of the black holes and black rings together with the corresponding black string quantities \tilde{A}_H^s , \tilde{T}_H^s , and \tilde{M}_H^s in Figure 12.

We note, that the EGB Schwarzschild black holes connect to the domain of existence of the EGB black rings only in the limit of Einstein gravity. Starting from this boundary point they form an infinite branch, otherwise disconnected from the black rings' domain of existence, with their scaled mass higher and their scaled area lower than the values possible for black rings.

In terms of the scaled coupling $\tilde{\alpha}'$, the domain of existence of the EGB black ring solutions is bounded on one side by the set of black ring solutions with the minimal (respectively maximal) values of b/a , while on the other side it is bounded by the set of EGB black string solutions. The two boundary lines merge and end in a cusp at the maximal scaled coupling $\tilde{\alpha}'$.

The presence of cusps in the sets of solutions typically signals a change of stability. The question of stability of the sets of solutions studied here is, however, beyond our current understanding. It would certainly be interesting to see whether the analogue of the Gregory-Laflamme instability [36] is present for EGB back strings and leads to associated sets of nonuniform EGB back strings. These latter would then be expected to be reflected in the emergence of new black rings, which are nonuniform along the S^1 . The presence of such solutions would give rise to a much more intricate EGB phase diagram (as would be presence of black Saturns, di-rings, etc.).

Moreover, it would be interesting to consider the phase diagram for dimensions higher than five. Construction of the uniform black strings would be straightforward, and one might observe a dimension dependence of the maximal GB coupling. Most intriguing would, however, be to find a possibility to obtain the corresponding sets of higher dimensional black rings.

5. Further remarks. Conclusions

In four spacetime dimensions, the Einstein-Hilbert action augmented by a cosmological constant term is the unique geometrical action (thus depending only on the metric and the curvature tensor) leading to field equations which involve at most second order derivatives of the metric. However, this is no longer true if the dimensionality of spacetime is greater than four, in which case, from a purely geometrical perspective, there is no compelling reason to consider only the Einstein-Hilbert action.

For $d = 5$, the most general theory of gravity leading to second order field equations for the metric is the EGB theory, which contains quadratic powers of the curvature. Although the solutions of this model have been studied for a long time, most of the literature considered only spherically symmetric configurations. Very few EGB exact solutions are known and none of them is axially symmetric.

In this paper we have argued that the approach used to construct $d = 5$ axially symmetric configurations in Einstein gravity within the Weyl formalism, can be used also for EGB solutions. This opens the possibility to generalize to EGB theory the known solutions with a nonspherical topology of the horizon.

Although it would clearly be preferable to have analytic solutions (if at all possible), we have made some progress in this direction by solving numerically the EGB equations. The main purpose of this work was to present a systematic analysis of the static black rings in EGB theory. The results of our investigation show that, for a given value of the GB coupling constant α' , the properties of the solutions are similar to their Einstein gravity counterparts. For example, all solutions we have found suffer from conical singularities and such solutions are presumably unstable. (The apparent unavoidable existence of conical singularities

plague all known asymptotically flat static solutions with a nonspherical topology of the horizon (including here also multi-black objects)). Interestingly, the absolute value of the conical excess decreases with the GB coupling constant α' , but the solutions stop to exist for some α'_{max} , before approaching a regular configuration.

The techniques proposed in this paper can easily be extended to other types of $d = 5$ static black objects in EGB theory (*e.g.* multi-black holes with S^3 topology of the horizon, black Saturns, di-rings). Another possible direction to approach in the future is the generalization of the results in Section 2 to the case of $d - 2$ commuting orthogonal Killing vector fields, with $d > 5$. However, these solutions will not be globally asymptotically flat. One way to construct $d > 5$ solutions approaching at infinity the Minkowski background and possessing a nonspherical topology of the horizon would be to extend the approach in the recent work [37] by including a GB term in the action.

Let us close this work by briefly mentioning the issue of charged static black rings in $d = 5$ EGB-Maxwell theory. One may hope that the inclusion of some matter fields will cure the conical singularity plaguing the vacuum solutions. The natural candidate here is a gauge field, in the simplest case an electromagnetic field. Soon after the discovery of the vacuum solution, an exact solution describing a U(1) electrically charged static black ring was found by several different authors [38], [7]. However, in Einstein-Maxwell theory, the presence of an electric charge alone was found insufficient to stabilize a static black ring and prevent it from collapsing, since conical singularities were unavoidable also in the charged case.

A priori, it is not obvious that this result holds also for EGB-Maxwell theory. Therefore we have considered a generalization of the EGB black ring solutions discussed in Section 4 by including a Maxwell term in the action (2.1). Since the Harrison-type generation techniques used to construct electrically charged solutions in Einstein-Maxwell theory do not hold in the presence of a GB term, one is constrained again to approach this problem numerically. Restricting ourselves to a purely electric U(1) potential, $A = V(\rho, z)dt$, we have performed for the charged case a similar computation to that described in Section 4. The boundary conditions satisfied by the metric functions are the same as before, while for the electric potential we have imposed $V(0, z) = \Phi$ (with Φ a constant) on the horizon and $\partial_\rho V(\rho, z)|_{\rho=0} = 0$ for the rest of the z -axis. At infinity, the electric potential vanishes, the electric charge being read from the asymptotic expansion of $V(\rho, z)$. The solutions were found starting with EGB configurations and slowly increasing the value for the electric potential on the horizon.

Although we did not explore yet systematically the full set of parameters, for all solutions we have found, the absolute value of the conical excess *increases* with Φ . Thus we conclude that the presence of an electric charge alone is very unlikely to stabilize the EGB black rings. Nonetheless, we expect that, similar to the Einstein-Maxwell theory, the conical singularities would be eliminated by submerging an EGB charged static black ring into a background gauge field. A drawback of this construction is that, due to the backreaction of the background electromagnetic field, the black ring will no longer be asymptotically flat.

However, the solutions in Section 3 may be viewed as an intermediate step towards the

construction of a rotating *balanced* black ring in EGB theory. In principle, the approach in this work can straightforwardly be generalized to the case of spinning solutions [40]. The only obstacle we can see at this moment is the tremendous complexity of the EGB equations in the presence of rotation.

Acknowledgements

B.K. gratefully acknowledges support by the DFG. The work of E.R. was supported by a fellowship from the Alexander von Humboldt Foundation.

A. The components of $G_{\mu\nu}$ and $H_{\mu\nu}$

For the metric ansatz (2.7), the essential nonvanishing components of the Einstein tensor G_{μ}^{ν} are:

$$G_{\rho}^{\rho} = e^{-2\nu} \left(-\dot{\nu}(\dot{U}_1 + \dot{U}_2 + \dot{U}_3) + \nu'(U_1' + U_2' + U_3') + \dot{U}_1^2 + \dot{U}_2^2 + \dot{U}_3^2 \right. \quad (\text{A.1})$$

$$\left. + (\nabla U_1) \cdot (\nabla U_2) + (\nabla U_1) \cdot (\nabla U_3) + (\nabla U_2) \cdot (\nabla U_3) + \ddot{U}_1 + \ddot{U}_2 + \ddot{U}_3 \right), \quad (\text{A.2})$$

$$G_z^z = e^{-2\nu} \left(-\nu'(U_1' + U_2' + U_3') + \dot{\nu}(\dot{U}_1 + \dot{U}_2 + \dot{U}_3) + U_1'^2 + U_2'^2 + U_3'^2 \right. \quad (\text{A.3})$$

$$\left. + (\nabla U_1) \cdot (\nabla U_2) + (\nabla U_1) \cdot (\nabla U_3) + (\nabla U_2) \cdot (\nabla U_3) + U_1'' + U_2'' + U_3'' \right),$$

$$G_z^{\rho} = e^{-2\nu} \left(\nu'(\dot{U}_1 + \dot{U}_2 + \dot{U}_3) + \dot{\nu}(U_1' + U_2' + U_3') - U_1' \dot{U}_1 - U_2' \dot{U}_2 - U_3' \dot{U}_3 - \dot{U}_1' - \dot{U}_2' - \dot{U}_3' \right), \quad (\text{A.4})$$

$$G_{\psi}^{\psi} = e^{-2\nu} \left((\nabla U_1)^2 + (\nabla U_3)^2 + (\nabla U_1) \cdot (\nabla U_3) + \nabla^2 \nu + \nabla^2 U_1 + \nabla^2 U_3 \right), \quad (\text{A.5})$$

$$G_{\varphi}^{\varphi} = e^{-2\nu} \left((\nabla U_1)^2 + (\nabla U_2)^2 + (\nabla U_1) \cdot (\nabla U_2) + \nabla^2 \nu + \nabla^2 U_1 + \nabla^2 U_2 \right), \quad (\text{A.6})$$

$$G_t^t = e^{-2\nu} \left((\nabla U_2)^2 + (\nabla U_3)^2 + (\nabla U_2) \cdot (\nabla U_3) + \nabla^2 \nu + \nabla^2 U_2 + \nabla^2 U_3 \right), \quad (\text{A.7})$$

The essential nonvanishing components of the tensor H_{μ}^{ν} are:

$$H_{\rho}^{\rho} = 4e^{-4\nu} \left(-\nu'(\dot{U}_1 \dot{U}_3 U_2' + \dot{U}_2 \dot{U}_3 U_1' + \dot{U}_2 \dot{U}_1 U_3') + \dot{\nu}(\dot{U}_3 U_1' U_2' + \dot{U}_2 U_1' U_3' + \dot{U}_1 U_2' U_3') \right. \quad (\text{A.8})$$

$$\left. - \dot{U}_1 \dot{U}_2 \dot{U}_3 (\dot{U}_1 + \dot{U}_2 + \dot{U}_3) + 3(\dot{\nu} \dot{U}_1 \dot{U}_2 \dot{U}_3 - \nu' U_1' U_2' U_3') - (\dot{U}_3^2 U_1' U_2' + \dot{U}_2^2 U_1' U_3' + \dot{U}_1^2 U_1' U_3') \right.$$

$$\left. - \ddot{U}_1 (\nabla U_2) \cdot (\nabla U_3) - \ddot{U}_2 (\nabla U_1) \cdot (\nabla U_3) - \ddot{U}_3 (\nabla U_2) \cdot (\nabla U_1) \right),$$

$$\begin{aligned}
H_z^z = 4e^{-4\nu} & \left(\nu'(\dot{U}_1\dot{U}_3U_2' + \dot{U}_2\dot{U}_3U_1' + \dot{U}_2\dot{U}_1U_3') - \dot{\nu}(\dot{U}_3U_1'U_2' + \dot{U}_2U_1'U_3' + \dot{U}_1U_2'U_3') \right. \\
& - U_1'U_2'U_3'(U_1' + U_2' + U_3') + 3(\nu'U_1'U_2'U_3' - \dot{\nu}\dot{U}_1\dot{U}_2\dot{U}_3) - (U_3'^2\dot{U}_1\dot{U}_2 + U_2'^2\dot{U}_1\dot{U}_3 + U_1'^2\dot{U}_2\dot{U}_3) \\
& \left. - U_1''(\nabla U_2) \cdot (\nabla U_3) - U_2''(\nabla U_1) \cdot (\nabla U_3) - U_3''(\nabla U_2) \cdot (\nabla U_1) \right), \tag{A.9}
\end{aligned}$$

$$\begin{aligned}
H_z^{\rho} = 4e^{-4\nu} & \left(-\nu'(\dot{U}_3U_1'U_2' + \dot{U}_2U_1'U_3' + \dot{U}_1U_2'U_3') - \dot{\nu}(\dot{U}_1\dot{U}_3U_2' + \dot{U}_3\dot{U}_2U_1' + \dot{U}_1\dot{U}_2U_3') \right. \\
& - 3(\nu'\dot{U}_1\dot{U}_2\dot{U}_3 + \dot{\nu}U_1'U_2'U_3') + (U_1'\dot{U}_1 + \dot{U}_1')(\nabla U_2) \cdot (\nabla U_3) \\
& \left. + (U_2'\dot{U}_2 + \dot{U}_2')(\nabla U_1) \cdot (\nabla U_3) + (U_3'\dot{U}_3 + \dot{U}_3')(\nabla U_2) \cdot (\nabla U_1) \right) \tag{A.10}
\end{aligned}$$

$$\begin{aligned}
H_{\psi}^{\psi} = 4e^{-4\nu} & \left(2(\nabla\nu)^2(\nabla U_1) \cdot (\nabla U_3) + \nu' \left(-(U_1' + U_3')(2\dot{U}_1\dot{U}_3 + U_1'U_3') + \dot{U}_3^2U_1' + \dot{U}_1^2U_3' \right) \right. \\
& + \dot{\nu} \left(-(\dot{U}_1 + \dot{U}_3)(2U_1'U_3' + \dot{U}_1\dot{U}_3) + U_3'^2\dot{U}_1 + U_1'^2\dot{U}_3 \right) - (U_1'\dot{U}_3 - U_3'\dot{U}_1)^2 \\
& - 2(U_3'\dot{\nu} + \dot{U}_3\nu' - \dot{U}_3U_3')\dot{U}_1' - 2(U_1'\dot{\nu} + \dot{U}_1\nu' - \dot{U}_1U_1')\dot{U}_3' + 2\dot{U}_1'\dot{U}_3' \\
& + (\dot{\nu}\dot{U}_3 - \nu'U_3')(U_1'' - \ddot{U}_1) + (\dot{\nu}\dot{U}_1 - \nu'U_1')(U_3'' - \ddot{U}_3) \\
& \left. - \ddot{U}_1U_3'^2 - U_1''\dot{U}_3^2 - \ddot{U}_3U_1'^2 - U_3''\dot{U}_1 - \ddot{U}_1U_3'' - U_1''\ddot{U}_3 - (\nabla U_1) \cdot (\nabla U_3)\nabla^2\nu \right), \tag{A.11}
\end{aligned}$$

$$\begin{aligned}
H_{\varphi}^{\varphi} = 4e^{-4\nu} & \left(2(\nabla\nu)^2(\nabla U_2) \cdot (\nabla U_1) + \nu' \left(-(U_1' + U_2')(2\dot{U}_2\dot{U}_1 + U_2'U_1') + \dot{U}_1^2U_2' + \dot{U}_2^2U_1' \right) \right. \\
& + \dot{\nu} \left(-(\dot{U}_1 + \dot{U}_2)(2U_2'U_1' + \dot{U}_2\dot{U}_1) + U_1'^2\dot{U}_2 + U_2'^2\dot{U}_1 \right) - (U_2'\dot{U}_1 - U_1'\dot{U}_2)^2 \\
& - 2(U_1'\dot{\nu} + \dot{U}_1\nu' - \dot{U}_1U_1')\dot{U}_2' - 2(U_2'\dot{\nu} + \dot{U}_2\nu' - \dot{U}_2U_2')\dot{U}_1' + 2\dot{U}_2'\dot{U}_1' \\
& + (\dot{\nu}\dot{U}_1 - \nu'U_1')(U_2'' - \ddot{U}_2) + (\dot{\nu}\dot{U}_2 - \nu'U_2')(U_1'' - \ddot{U}_1) - \ddot{U}_2U_1'^2 - U_2''\dot{U}_1^2 - \ddot{U}_1U_2'^2 - U_1''\dot{U}_2^2 \\
& \left. - \ddot{U}_2U_1'' - U_2''\ddot{U}_1 - (\nabla U_1) \cdot (\nabla U_2)\nabla^2\nu \right), \tag{A.12}
\end{aligned}$$

$$\begin{aligned}
H_t^t = 4e^{-4\nu} & \left(2(\nabla\nu)^2(\nabla U_3) \cdot (\nabla U_2) + \nu' \left(-(U_2' + U_3')(2\dot{U}_3\dot{U}_2 + U_3'U_2') + \dot{U}_2^2U_3' + \dot{U}_3^2U_2' \right) \right. \\
& + \dot{\nu} \left(-(\dot{U}_2 + \dot{U}_3)(2U_3'U_2' + \dot{U}_3\dot{U}_2) + U_2'^2\dot{U}_3 + U_3'^2\dot{U}_2 \right) - (U_3'\dot{U}_2 - U_2'\dot{U}_3)^2 \\
& - 2(U_2'\dot{\nu} + \dot{U}_2\nu' - \dot{U}_2U_2')\dot{U}_3' - 2(U_3'\dot{\nu} + \dot{U}_3\nu' - \dot{U}_3U_3')\dot{U}_2' + 2\dot{U}_3'\dot{U}_2' \\
& + (\dot{\nu}\dot{U}_2 - \nu'U_2')(U_3'' - \ddot{U}_3) + (\dot{\nu}\dot{U}_3 - \nu'U_3')(U_2'' - \ddot{U}_2) - \ddot{U}_3U_2'^2 - U_3''\dot{U}_2^2 \\
& \left. - \ddot{U}_2U_3'^2 - U_2''\dot{U}_3^2 - \ddot{U}_3U_2'' - \ddot{U}_2U_3'' - (\nabla U_3) \cdot (\nabla U_2)\nabla^2\nu \right), \tag{A.13}
\end{aligned}$$

where we define

$$(\nabla U) \cdot (\nabla V) = \partial_{\rho}U\partial_{\rho}V + \partial_zU\partial_zV, \quad \nabla^2U = \partial_{\rho}^2U + \partial_z^2U, \tag{A.14}$$

The expressions of these tensors in terms of the functions f_i is straightforward.

In practice we have solved the following combination of the EGB equations

$$E_\rho^\rho + E_z^z + E_\psi^\psi + E_\varphi^\varphi - 2E_t^t = 0, \quad E_\rho^\rho + E_z^z - 2E_\psi^\psi + E_\varphi^\varphi + E_t^t = 0, \quad (\text{A.15})$$

$$E_\rho^\rho + E_z^z + E_\psi^\psi - 2E_\varphi^\varphi + E_t^t = 0, \quad E_\rho^\rho + E_z^z - \frac{1}{2}(E_\psi^\psi + E_\varphi^\varphi + E_t^t) = 0, \quad (\text{A.16})$$

which diagonalizes the Einstein tensor w.r.t. $\nabla^2 U_1, \nabla^2 U_2, \nabla^2 U_3$ and respectively $\nabla^2 \nu$.

B. Details on the numerics

B.1 A new coordinate system

Although we could construct²¹ EGB black ring solutions by employing the Weyl-type coordinates (ρ, z) , the metric ansatz (2.12) has a number of disadvantages. For example, it has proven difficult to extract with enough accuracy the value of the mass parameter M from the asymptotic form of f_0 and also to study solutions with $a/b \rightarrow 0$ or $a/b \rightarrow 1$.

To solve numerically the EGB equations, we have found it more convenient to introduce the new coordinates r, θ and reparametrize the metric (2.12) as

$$ds^2 = -\hat{f}_0(r, \theta) dt^2 + \frac{1}{\hat{f}_1(r, \theta)} (dr^2 + r^2 d\theta^2) + \frac{\hat{f}_2(r, \theta)}{\hat{f}_3(r, \theta)} d\psi^2 + \hat{f}_3(r, \theta) d\varphi^2, \quad (\text{B.1})$$

$$r_0 \leq r < \infty, \quad 0 \leq \theta \leq \frac{\pi}{2}, \quad (\text{B.2})$$

where (ρ, z) are related to (r, θ) by²²

$$\rho = \frac{r^4 - r_0^4}{2r^2} \sin 2\theta, \quad z = \frac{r^4 + r_0^4}{2r^2} \cos 2\theta, \quad (\text{B.3})$$

with $r_0^2 = a$. In these coordinates the horizon is located at $r = r_0, 0 \leq \theta \leq \frac{\pi}{2}$. The semi-finite and finite ψ -rods are mapped to $r_0 \leq r < \infty, \theta = \pi/2$ and $r_0 \leq r \leq r_b, \theta = 0$, respectively, while the semi-finite φ -rod is on the interval $r_b \leq r < \infty, \theta = 0$. Here $r_b = \sqrt{b + \sqrt{b^2 - a^2}}$.

Next we introduce background functions \hat{f}_i^0

$$\hat{f}_i = \hat{f}_i^0 \hat{F}_i, \quad (\text{B.4})$$

analogous to Eq. (4.6). Note that in the coordinates (r, θ) the background functions \hat{f}_0^0, \hat{f}_2^0 simplify to

$$\hat{f}_0^0 = \left(\frac{r^2 - r_0^2}{r^2 + r_0^2} \right)^2, \quad \hat{f}_2^0 = \left(\frac{r^2 + r_0^2}{r} \right)^4 \cos^2 \theta \sin^2 \theta,$$

²¹The methods in this case were similar to those used in [37] to construct $d = 6, 7$ black holes with $S^2 \times S^{d-4}$ topology of the horizon.

²²Note that this coordinate transformation reduces to (2.15) for $r_0 = 0$.

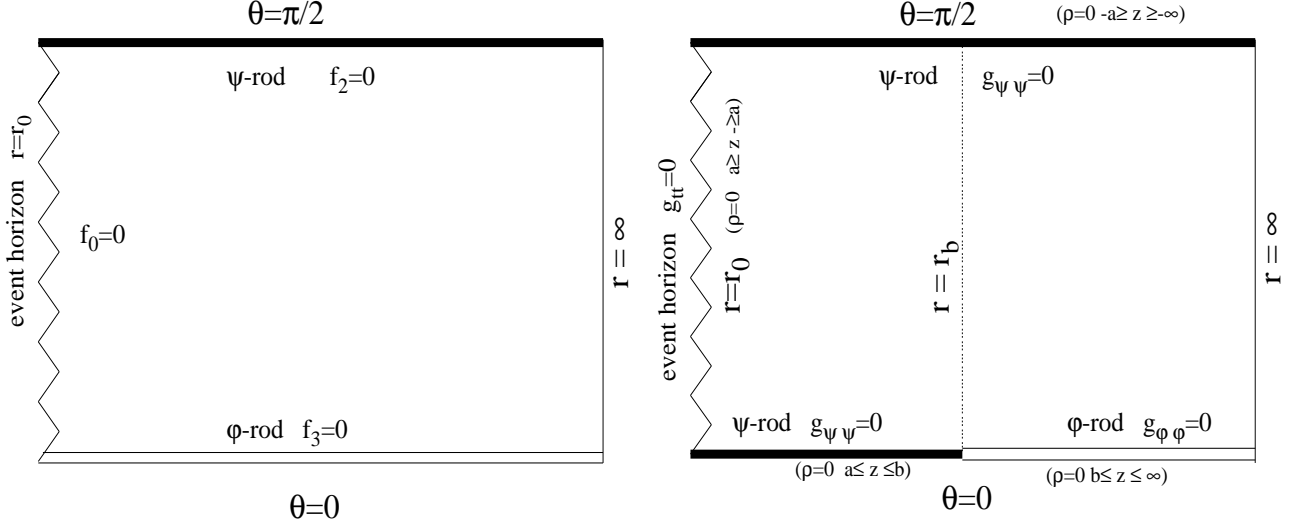


Figure 13. The domain of integration for the coordinate system (B.1) is shown for a EGB Schwarzschild black hole (left) and a static black ring (right). The relation with the Weyl-type coordinates in (2.12) is also presented.

and \hat{f}_1^0 is regular and finite except at the intersection of the ψ -rod and the φ -rod. For completeness we also include the background functions \hat{f}_1^0 and \hat{f}_3^0

$$\hat{f}_1^0 = \frac{2R_3}{r^2} \left(\frac{1 + \left(\frac{r_0}{r_b}\right)^2}{1 + \left(\frac{r_0}{r}\right)^2} \right)^2 \left[\left(1 + \left(\frac{r_0}{r_b}\right)^4\right) \left(1 + \left(\frac{r_0}{r}\right)^4\right) + 4 \left(\frac{r_0}{r_b}\right)^2 \left(\frac{R_3}{r^2} - \left(\frac{r_0}{r}\right)^2 \cos 2\theta\right) \right]^{-1},$$

$$\hat{f}_3^0 = \frac{1}{2} \left(2R_3 + r_b^2 \left(1 + \left(\frac{r_0}{r_b}\right)^4 - \left(\frac{r_0}{r_b}\right)^2 \cos 2\theta \left[\left(\frac{r_0}{r}\right)^2 + \left(\frac{r}{r_0}\right)^2 \right] \right) \right),$$

where

$$R_3 = \frac{r^2}{2} \left[\left(1 + \left(\frac{r_b}{r}\right)^4 - 2 \cos 2\theta \left(\frac{r_b}{r}\right)^2 \right) \left(1 + \left(\frac{r_0^2}{rr_b}\right)^4 - 2 \cos 2\theta \left(\frac{r_0^2}{rr_b}\right)^2 \right) \right]^{1/2}.$$

The black hole limit corresponds to $r_b = r_a$, in which case one can easily see that the EGB Schwarzschild black hole written in isotropic coordinates is recovered. The relation between the coordinates in the new metric form (B.1) and the Weyl ones in (2.12) is shown in Figure 13 for both black holes and black rings solutions.

The boundary conditions for the functions \hat{F}_i follow from the expansions Eqs. (2.18), (2.19) and the assumption of asymptotic flatness. Thus $\hat{F}_i \rightarrow 1$ as $r \rightarrow \infty$ and the normal derivatives of all functions vanish on the other boundaries, except $\hat{F}_1 \hat{F}_3 = 1$ along $\theta = 0$, $r_b \leq r < \infty$.

B.2 The numerical methods

With these parametrisation we solve the resulting set of four coupled non-linear elliptic partial differential equations numerically, subject to the above boundary conditions.

First, one introduces the new radial variable $x = 1 - r_0/r$ which maps the semi infinite region $[r_0, \infty)$ to the closed region $[0, 1]$. This leads to the following substitutions in the differential equations

$$r\hat{F}_{,r} \longrightarrow (1-x)\hat{F}_{,x} \quad r^2\hat{F}_{,rr} \longrightarrow (1-x)^2\hat{F}_{,xx} - 2(1-x)\hat{F}_{,x} \quad (\text{B.5})$$

for any function \hat{F}_i .

The equations for \hat{F}_i are then discretized on a non-equidistant grid in x and θ . Typical grids used have sizes 90×50 , covering the integration region $0 \leq x \leq 1$ and $0 \leq \theta \leq \pi/2$.

All numerical calculations are performed by using the programs FIDISOL/CADSOL, which uses a Newton-Raphson method. A detailed presentation of the this code is presented in [39]. This code requests the system of nonlinear partial differential equations to be written in the form $P(x, \theta, u, u_x, u_\theta, u_{x\theta}, u_{xx}, u_{\theta\theta}) = 0$, (where u denotes the set of unknown functions) subject to a set of boundary conditions on a rectangular domain. The user must deliver to FIDISOL/CADSOL the equations, the boundary conditions, the Jacobian matrices for the equations and the boundary conditions, and some initial guess functions. The numerical procedure works as follows: for an approximate solution $u^{(1)}$, $P(u^{(1)})$ does not vanish. The next step is to consider an improved solution $u^{(2)} = u^{(1)} + \Delta u$, supposing that $P(u^{(1)} + \Delta u) = 0$. The expansion in the small parameter Δu gives in the first order $0 = P(u^{(1)} + \Delta u) \approx P(u^{(1)}) + \frac{\partial P}{\partial u}(u^{(1)})\Delta u + \frac{\partial P}{\partial u_x}(u^{(1)})\Delta u_x + \dots$. This equation can be used to determine the correction $\Delta u^{(1)} = \Delta u$. Repeating the calculations iteratively ($u^{(3)} = u^{(2)} + \Delta u^{(2)}$ etc), the approximate solutions will converge, provided the initial guess solution is close enough to the exact solution. The iteration stops after i steps if the Newton residual $P(u^{(i)})$ is smaller than a prescribed tolerance. Therefore it is essential to have a good first guess, to start the iteration procedure.

In each iteration step a correction to the initial guess configuration is computed. The maximum of the relative defect decreases by a factor of 20 from one iteration step to another. However, for large values of α' convergence is slower. In this case we re-iterate the solution until the defect is small enough (about 10^{-4}). Note, that this defect concerns the discretized equations. The estimates of the relative error of the solution (truncation error) are computed separately. They are of the order 0.001. The errors also depend on the order of consistency of the method, *i.e.* on the order of the discretisation of derivatives. For the solutions in this paper, this order was six. We have also monitored the quantities

$$n_{(k)} = \left(\sum_i e_{(k)}^2(x_i, \theta_i) \right)^{1/2}, \quad (\text{B.6})$$

(with x_i, θ_i a point of the mesh and $e_{(k)}$ a discretized equation), which provide an average error estimate. For most of the solutions, we have found $n_{(k)} < 10^{-11}$ (this holds also for the constraint equations E_r^θ and $E_r^r - E_\theta^\theta$). Most of the errors come from the region around the point $r = r_b$, $\theta = 0$, where the distribution of the points in the mesh should be carefully chosen.

In this scheme, the input parameters are the positions of the rods fixed by a and b , (resp. r_0 and r_b) and the value α' of the GB coupling parameter. To obtain EGB

black rings, one starts with the Einstein gravity solution as initial guess (*i.e.* $\alpha' = 0$ and $F_i = 1$) and increases the value of α' slowly. The iterations converge, and, in principle, repeating the procedure one obtains in this way solutions for higher α' . For some of the configurations, we interpolate the resulting configurations and use them as a starting guess on a finer grid.

The mass M of the solutions can be determined by extracting the coefficient of the $1/r^2$ decay of the metric component g_{tt}

$$-g_{tt} \rightarrow 1 - c_0/r^2, \quad (\text{B.7})$$

with $c_0 = 16\pi GM/3V_3$. Alternatively, the Smarr-like relation (4.10) between mass, surface area, Hawking temperature, and the integral $I_{\alpha'}$ can be employed to determine the mass once the other quantities are computed. Comparing this Smarr value for the mass with the mass evaluated from the asymptotic decay we find excellent agreement, *i. e.* deviations occur only after 6 digits.

B.3 The issue of the maximal value of α'

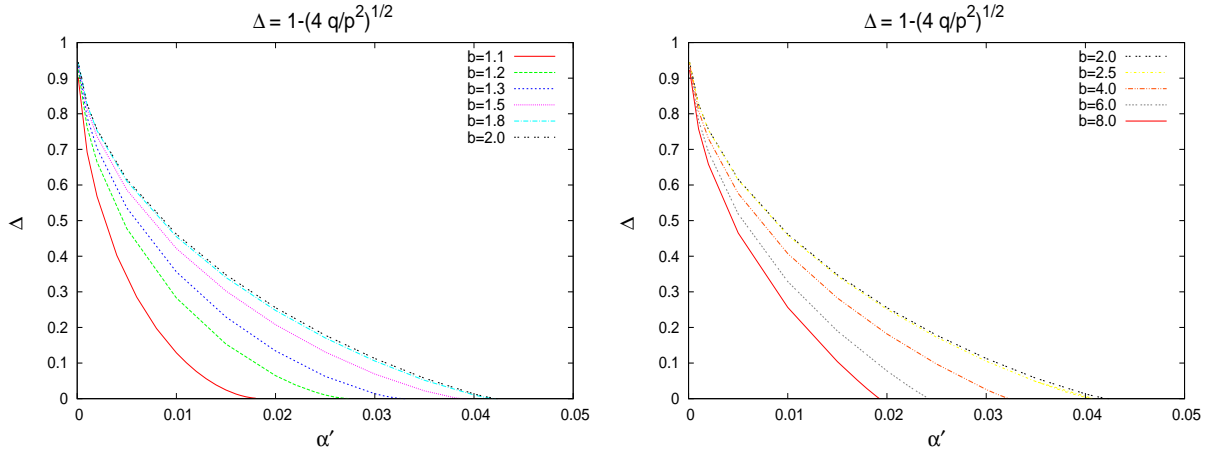


Figure 14. The discriminant Δ is shown as a function α' for several values of the ratio b/a .

When α' approaches its maximal value, no singularity shows up. In order to get more insight into this behaviour we follow the approach of ref. [20] and study the expansion of the solution near $(r = r_0, \theta = 0)$.

Defining $\eta = r - r_0$ we parametrise the solution as

$$\begin{aligned} \hat{f}_0 &= \eta^2 \left[(h_0 + h_{0,r}\eta + h_{0,rr}\eta^2) + (h_{0,\theta\theta} + h_{0,r\theta\theta}\eta + h_{0,rr\theta\theta}\eta^2) \frac{\theta^2}{2} \right], \\ \hat{f}_1 &= (h_1 + h_{1,r}\eta + h_{1,rr}\eta^2) + (h_{1,\theta\theta} + h_{1,r\theta\theta}\eta + h_{1,rr\theta\theta}\eta^2) \frac{\theta^2}{2}, \\ \hat{f}_2 &= (h_2 + h_{2,r}\eta + h_{2,rr}\eta^2) \frac{\theta^2}{2} + (h_{2,\theta\theta} + h_{2,r\theta\theta}\eta + h_{2,rr\theta\theta}\eta^2) \frac{\theta^4}{24}, \\ \hat{f}_3 &= (h_3 + h_{3,r}\eta + h_{3,rr}\eta^2) + (h_{3,\theta\theta} + h_{3,r\theta\theta}\eta + h_{3,rr\theta\theta}\eta^2) \frac{\theta^2}{2}, \end{aligned}$$

where already the boundary conditions at $\theta = 0$ have been taken into account. Here the quantities $h_{i,\mu\nu\dots}$ denote constants (in abuse of notation).

Substitution in the EGB equations yields for the first order expansion coefficients

$$\begin{aligned} h_{0,r} &= -h_0/r_0, & h_{0,r\theta\theta} &= -h_{0,\theta\theta}/r_0, & h_{1,r} &= -2h_0/r_0, & h_{1,\theta\theta} &= -h_{0,\theta\theta}\frac{h_1}{h_0}, \\ h_{1,r\theta\theta} &= -2h_{0,\theta\theta}/r_0\frac{h_1}{h_0}, & h_{2,r} &= 0, & h_{3,r} &= 0, & h_{3,r\theta\theta} &= 0 \end{aligned}$$

For the second order expansion coefficients $h_{i,rr}$ we find a system of quadratic equations. After some algebra we find for the coefficients $h_{1,rr}$ an equations of the form

$$h_{1,rr}^2 + ph_{1,rr} + q = 0. \quad (\text{B.8})$$

The coefficients $h_{0,rr}$, $h_{2,rr}$ and $h_{3,rr}$ can be expressed in terms of $h_{1,rr}$.

The discriminant of Eq. (B.8) is given by

$$\frac{p^2}{4} - q = \frac{[2((8h_2h_{3,\theta\theta} - h_{2,\theta\theta}h_3)h_0 + 2h_2h_3h_{0,\theta\theta})(2\alpha'h_{3,\theta\theta} - h_3h_1r_0^2)\alpha' + h_0h_2h_3^2h_1^2r_0^4]h_1^4}{64[2\alpha'h_{3,\theta\theta} - h_1h_3r_0^2]^2\alpha'^2h_0h_2}. \quad (\text{B.9})$$

A real solution to Eq. (B.8) exists only if $\frac{p^2}{4} - q \geq 0$. We monitored the discriminant and observed that the solutions cease to exist exactly when the discriminant becomes negative. This is demonstrated in Figure 14.

References

- [1] R. Emparan and H. S. Reall, Phys. Rev. Lett. **88** (2002) 101101 [arXiv:hep-th/0110260].
- [2] R. Emparan and H. S. Reall, Phys. Rev. D **65** (2002) 084025 [arXiv:hep-th/0110258].
- [3] R. C. Myers and M. J. Perry, Annals Phys. **172** (1986) 304.
- [4] H. Elvang, Phys. Rev. D **68** (2003) 124016 [arXiv:hep-th/0305247].
- [5] R. Emparan, JHEP **0403** (2004) 064 [arXiv:hep-th/0402149].
- [6] H. Elvang, R. Emparan, D. Mateos and H. S. Reall, Phys. Rev. Lett. **93** (2004) 211302 [arXiv:hep-th/0407065].
- [7] H. K. Kunduri and J. Lucietti, Phys. Lett. B **609** (2005) 143 [arXiv:hep-th/0412153].
- [8] B. Chng, R. Mann, E. Radu and C. Stelea, JHEP **0812** (2008) 009 [arXiv:0809.0154 [hep-th]].
- [9] H. Elvang and P. Figueras, JHEP **0705** (2007) 050 [arXiv:hep-th/0701035].
- [10] H. Elvang and M. J. Rodriguez, JHEP **0804** (2008) 045 [arXiv:0712.2425 [hep-th]].
- [11] K. Izumi, Prog. Theor. Phys. **119** (2008) 757 [arXiv:0712.0902 [hep-th]].
- [12] H. Iguchi and T. Mishima, Phys. Rev. D **75** (2007) 064018 [arXiv:hep-th/0701043].
- [13] J. Evslin and C. Krishnan, Class. Quant. Grav. **26** (2009) 125018 arXiv:0706.1231 [hep-th].
- [14] J. P. Gauntlett and J. B. Gutowski, Phys. Rev. D **71** (2005) 025013 [arXiv:hep-th/0408010];
J. P. Gauntlett and J. B. Gutowski, Phys. Rev. D **71** (2005) 045002 [arXiv:hep-th/0408122].

- [15] D. J. Gross and E. Witten, Nucl. Phys. B **277** (1986) 1;
R. R. Metsaev and A. A. Tseytlin, Phys. Lett. B **191** (1987) 354;
C. G. Callan, R. C. Myers, and M. J. Perry, Nucl. Phys. **B311** (1988) 673.
- [16] R. C. Myers, Phys. Rev. D **36** (1987) 392.
- [17] C. Garraffo and G. Giribet, Mod. Phys. Lett. A **23** (2008) 1801 [arXiv:0805.3575 [gr-qc]].
- [18] C. Charmousis, Lect. Notes Phys. **769** (2009) 299 [arXiv:0805.0568 [gr-qc]].
- [19] D. G. Boulware and S. Deser, Phys. Rev. Lett. **55** (1985) 2656;
J. T. Wheeler, Nucl. Phys. B **268** (1986) 737.
- [20] T. Kobayashi and T. Tanaka, Phys. Rev. D **71** (2005) 084005 [arXiv:gr-qc/0412139].
- [21] G. W. Gibbons and S. W. Hawking, Phys. Rev. D **15** (1977) 2752.
- [22] T. Harmark, Phys. Rev. D **70** (2004) 124002 [arXiv:hep-th/0408141].
- [23] S. Hollands and S. Yazadjiev, Commun. Math. Phys. **283** (2008) 749 [arXiv:0707.2775 [gr-qc]].
- [24] E. Sorkin, B. Kol and T. Piran, Phys. Rev. D **69** (2004) 064032 [arXiv:hep-th/0310096].
- [25] H. Kudoh and T. Wiseman, Prog. Theor. Phys. **111** (2004) 475 [arXiv:hep-th/0310104].
- [26] T. Wiseman, Class. Quant. Grav. **20** (2003) 1137 [arXiv:hep-th/0209051].
- [27] B. Kleihaus, J. Kunz and E. Radu, JHEP **0606** (2006) 016 [arXiv:hep-th/0603119].
- [28] S. Deser and B. Tekin, Phys. Rev. D **67** (2003) 084009 [arXiv:hep-th/0212292];
A. Padilla, Class. Quant. Grav. **20** (2003) 3129 [arXiv:gr-qc/0303082];
S. Deser and B. Tekin, Phys. Rev. D **75** (2007) 084032 [arXiv:gr-qc/0701140];
D. Kastor, Class. Quant. Grav. **25** (2008) 175007 [arXiv:0804.1832 [hep-th]];
N. Deruelle, J. Katz and S. Ogushi, Class. Quant. Grav. **21** (2004) 1971
[arXiv:gr-qc/0310098].
- [29] S. W. Hawking in *General Relativity. An Einstein Centenary Survey*, edited by
S. W. Hawking and W. Israel, (Cambridge, Cambridge University Press, 1979).
- [30] D. Astefanesei and E. Radu, Phys. Rev. D **73** (2006) 044014 [arXiv:hep-th/0509144].
- [31] M. S. Costa and M. J. Perry, Nucl. Phys. B **591** (2000) 469 [arXiv:hep-th/0008106].
- [32] D. V. Fursaev and S. N. Solodukhin, Phys. Rev. D **52** (1995) 2133 [arXiv:hep-th/9501127].
- [33] R. M. Wald, Phys. Rev. D **48** (1993) 3427 [arXiv:gr-qc/9307038].
- [34] C. Herdeiro, B. Kleihaus, J. Kunz and E. Radu, *On the Bekenstein-Hawking area law for
black objects with conical singularities*, in preparation.
- [35] M. Azreg-Ainou and G. Clement, Class. Quant. Grav. **13** (1996) 2635 [arXiv:gr-qc/9603059].
- [36] R. Gregory and R. Laflamme, Phys. Rev. Lett. **70** (1993) 2837 [arXiv:hep-th/9301052].
- [37] B. Kleihaus, J. Kunz and E. Radu, Phys. Lett. B **678** (2009) 301 [arXiv:0904.2723 [hep-th]].
- [38] D. Ida and Y. Uchida, Phys. Rev. D **68**, 104014 (2003) [arXiv:gr-qc/0307095];
S. S. Yazadjiev, arXiv:hep-th/0507097.
- [39] W. Schönauer and R. Weiß, J. Comput. Appl. Math. **27**, 279 (1989) 279;
M. Schauder, R. Weiß and W. Schönauer, The CADSOL Program Package, Universität
Karlsruhe, Interner Bericht Nr. 46/92 (1992).
- [40] B. Kleihaus, J. Kunz and E. Radu, in preparation.